

The 10<sup>th</sup> China LHC Physics Conference (CLHCP2024)

第十届中国LHC物理会议

# Probe nuclear structure in high energy nuclear collisions

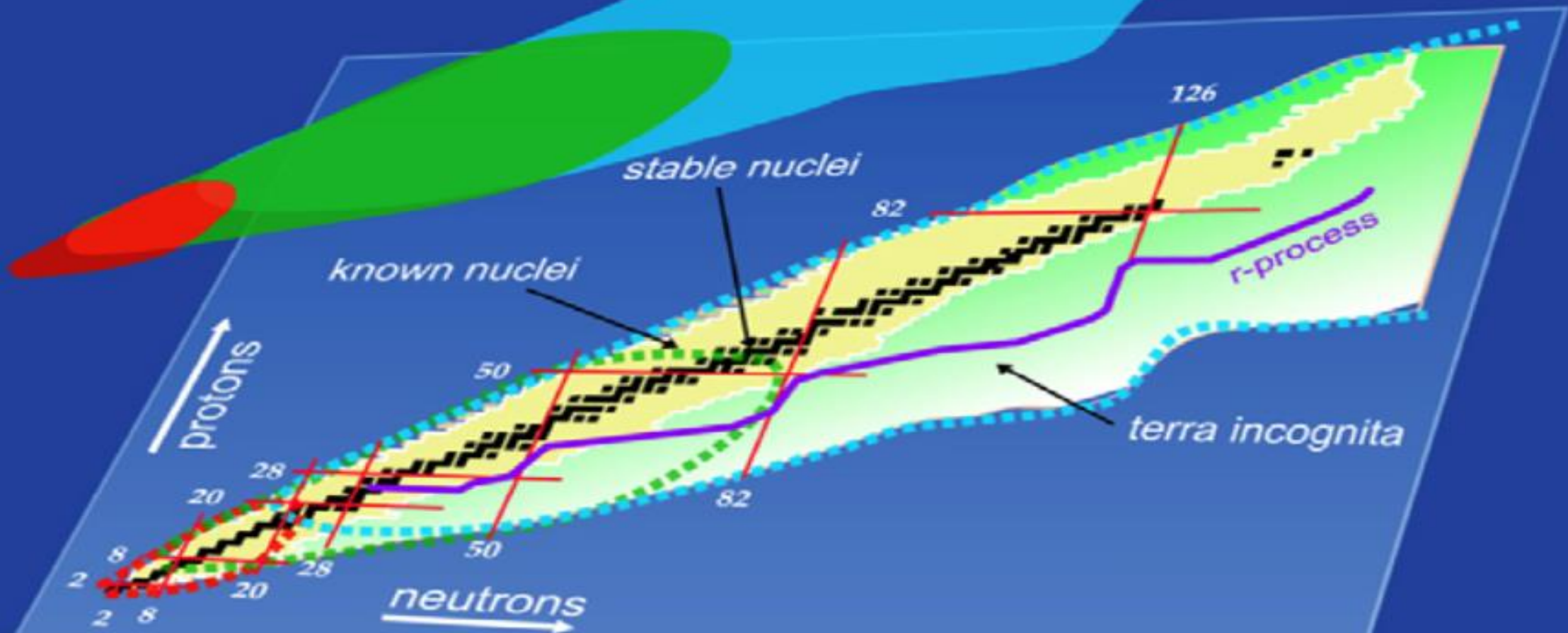
Chunjian Zhang (张春健)

Fudan University

Nov. 16<sup>th</sup>, 2024, Qingdao

# Nuclear Landscape

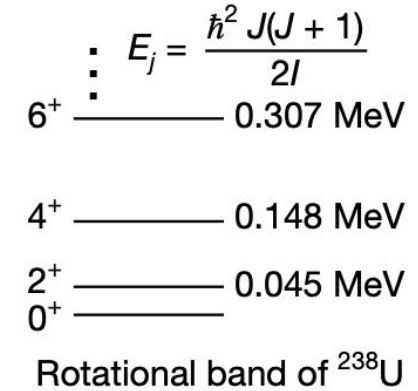
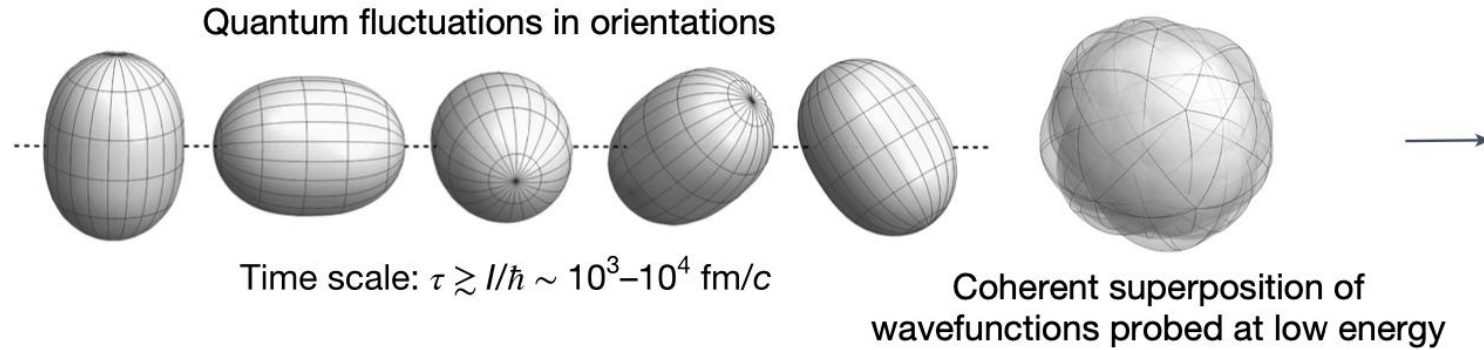
- Ab initio
- Configuration Interaction
- Density Functional Theory





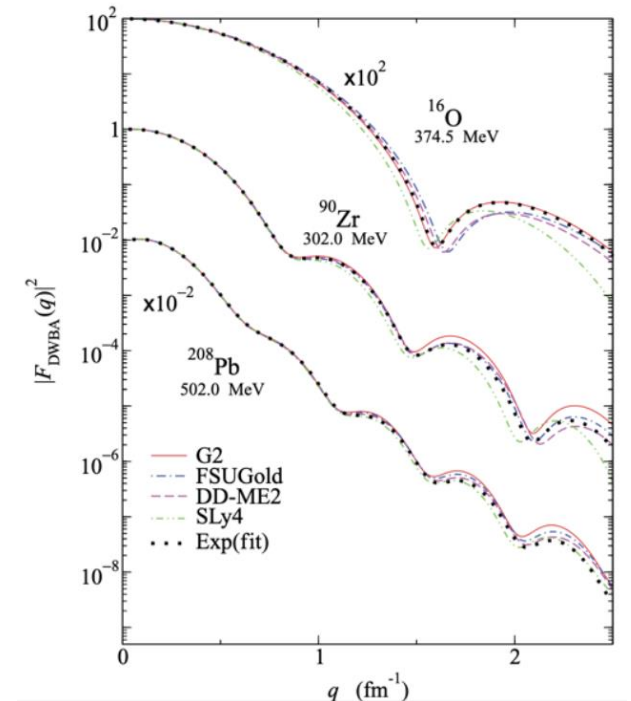
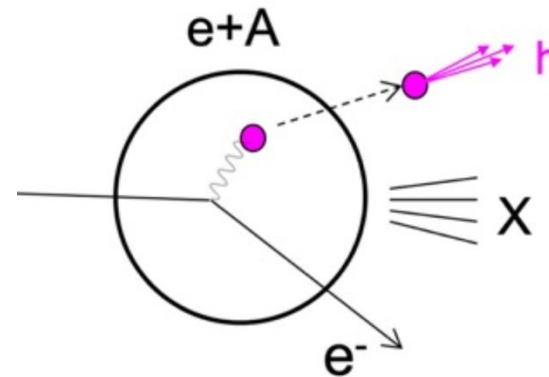
# Nuclear shape in lower energy method

Each DOF has zero-point fluctuations within an intrinsic timescale.



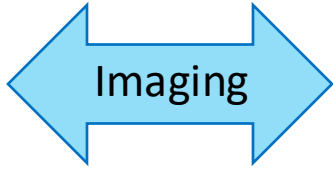
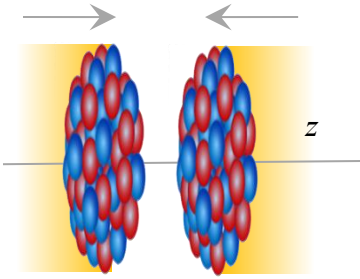
(non-invasive) spectroscopic methods probe a superposition of these fluctuations  
 Instantaneous nuclear shapes are not directly seen → intrinsic shape not observable

e+A scattering has very short timescales, but so far mostly imaged the one-body (charge) distribution.  
 The impact of deformation appears as an increase in the radius

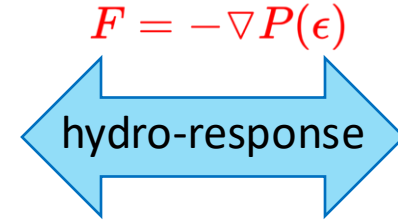
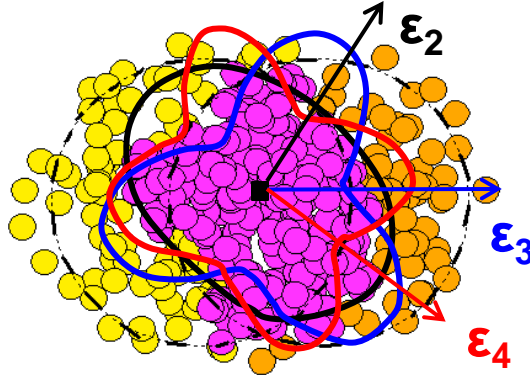


# Collective flow-assisted nuclear structure imaging

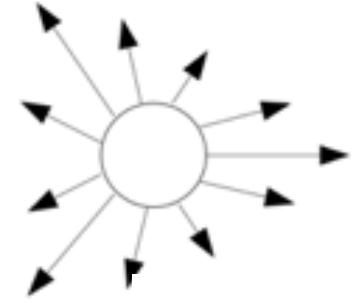
## Nuclear structure



## Initial conditions



## Final state



$$\rho(r, \theta, \phi) = \frac{\rho_0}{1 + e^{(r-R(\theta, \phi))/a_0}}$$

$$R(\theta, \phi) = R_0(1 + \beta_2[\cos \gamma Y_{2,0}(\theta, \phi) + \sin \gamma Y_{2,2}(\theta, \phi)] + \beta_3 Y_{3,0}(\theta, \phi))$$

- $\beta_2 \rightarrow$  Quadrupole deformation
- $\beta_3 \rightarrow$  Octupole deformation
- $\gamma \rightarrow$  Triaxiality
- $a_0 \rightarrow$  Surface diffuseness
- $R_0 \rightarrow$  Nuclear size

Many-body correlations

### Initial Size

$$R_{\perp}^2 \propto \langle r_{\perp}^2 \rangle$$

### Initial Shape

$$\mathcal{E}_n \propto \langle r_{\perp}^n e^{in\phi} \rangle$$

$R_0$

$a_0$

$\beta_n$

?

### Radial Flow

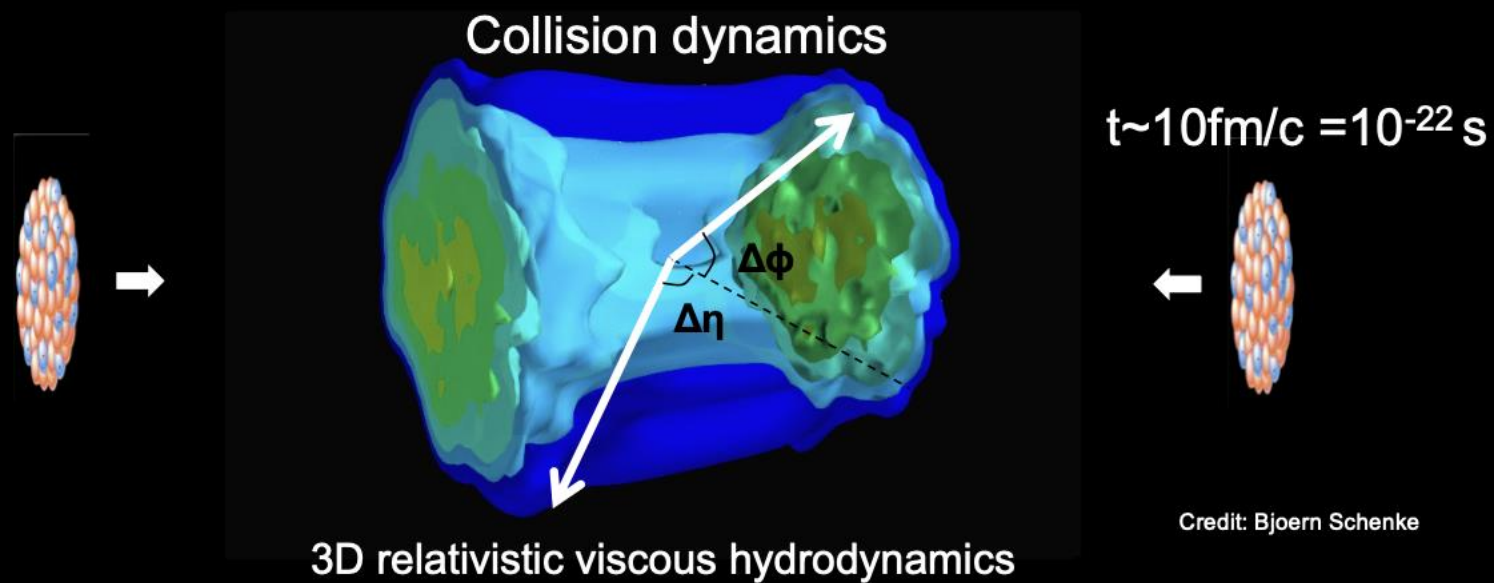
### Anisotropic Flow

$$\frac{d^2 N}{d\phi dp_T} = N(p_T) \left( \sum_n V_n e^{-in\phi} \right)$$

$$N_{ch} \propto N_{part} \quad \frac{\delta[p_T]}{[p_T]} \propto -\frac{\delta R_{\perp}}{R_{\perp}} \quad V_n \propto \mathcal{E}_n$$

High energy: Large multiplicity and boost invariance; approximate linear response in each event

Key: 1) fast snapshot, 2) linear response, 3) large multiplicity for many body correlation



Relativistic viscous Hydrodynamics (first-order):

Energy momentum conservation laws

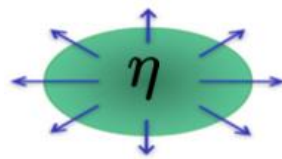
$$\partial_\mu T^{\mu\nu} = 0$$

$$T^{\mu\nu} = \underbrace{\epsilon u^\mu u^\nu}_{\text{Equation-of-state } P(\epsilon)} - \underbrace{(P + \Pi)}_{\text{Bulk pressure}} \Delta^{\mu\nu} + \underbrace{\pi^{\mu\nu}}_{\text{Shear tensor}}$$

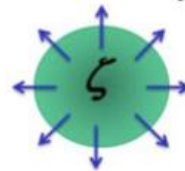
$$\pi^{\mu\nu} = -\eta \sigma^{\mu\nu} \quad \eta: \text{shear viscosity} \quad \Pi = -\zeta \nabla_\lambda^\perp u^\lambda \quad \zeta: \text{bulk viscosity}$$

1) Collective flow driven by QCD EoS:  $F = -\nabla P(\epsilon)$

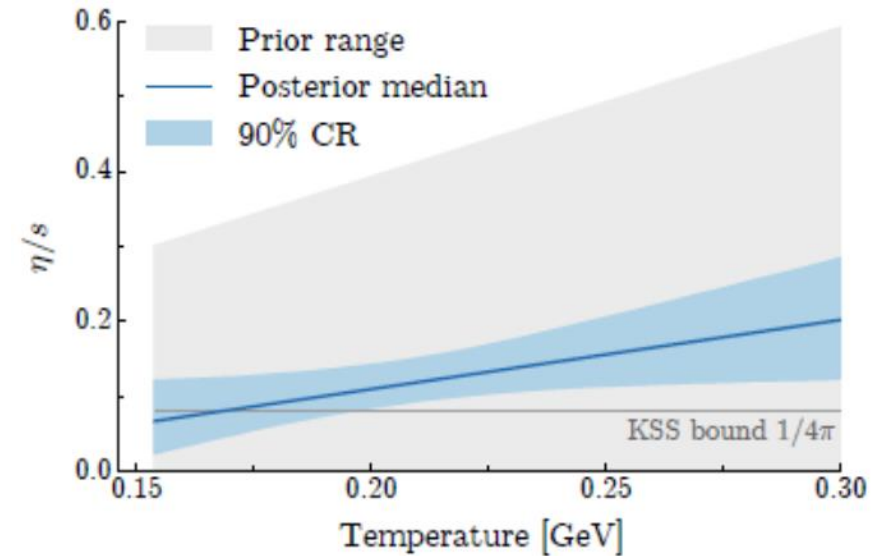
2) But resisted by viscosity



Reduce anisotropic flow



Reduce radial flow



A quantitative extraction of the QGP viscosity:  $\eta/s$  (T) is very close to the ADS/CFT bound of  $1/4\pi$

$$\mathcal{E}_2 \equiv \varepsilon_2 e^{2i\Phi_2} \propto \int_{\mathbf{r}} \mathbf{r}^2 \rho(\mathbf{r}) \quad d_{\perp} = 1/R_{\perp} \quad \delta d_{\perp} = d_{\perp} - \langle d_{\perp} \rangle$$

- We measure moments of  $p(1/R, \varepsilon_2, \varepsilon_3 \dots)$  via  $p([p_T], v_2, v_3 \dots)$ ...

■ Mean	$\langle d_{\perp} \rangle$	$\langle p_T \rangle$
■ Variance:	$\langle \varepsilon_n^2 \rangle, \langle (\delta d_{\perp}/d_{\perp})^2 \rangle$	$\langle v_n^2 \rangle, \langle (\delta p_T/p_T)^2 \rangle$
■ Skewness	$\langle \varepsilon_n^2 \delta d_{\perp}/d_{\perp} \rangle, \langle (\delta d_{\perp}/d_{\perp})^3 \rangle$	$\langle v_n^2 \delta p_T/p_T \rangle, \langle (\delta p_T/p_T)^3 \rangle$
■ Kurtosis	$\langle \varepsilon_n^4 \rangle - 2\langle \varepsilon_n^2 \rangle^2, \langle (\delta d_{\perp}/d_{\perp})^4 \rangle - 3\langle (\delta d_{\perp}/d_{\perp})^2 \rangle^2$	$\langle v_n^4 \rangle - 2\langle v_n^2 \rangle^2, \langle (\delta p_T/p_T)^4 \rangle - 3\langle (\delta p_T/p_T)^2 \rangle^2$
...		

- Higher moments probe the frame-independent many-body distributions

$$\langle \varepsilon_2^2 \rangle = \langle \mathcal{E}_2 \mathcal{E}_2^* \rangle \approx \frac{\int_{\mathbf{r}_1, \mathbf{r}_2} (\mathbf{r}_1)^2 (\mathbf{r}_2^*)^2 \rho(\mathbf{r}_1, \mathbf{r}_2)}{(\int_{\mathbf{r}} |\mathbf{r}|^2 \langle \rho(\mathbf{r}) \rangle)^2} \quad \langle \varepsilon_2^2 \delta d_{\perp}/d_{\perp} \rangle \approx - \frac{\int_{\mathbf{r}_1, \mathbf{r}_2, \mathbf{r}_3} (\mathbf{r}_1)^2 (\mathbf{r}_2^*)^2 |\mathbf{r}_3|^2 \rho(\mathbf{r}_1, \mathbf{r}_2, \mathbf{r}_3)}{(\int_{\mathbf{r}} |\mathbf{r}|^2 \langle \rho(\mathbf{r}) \rangle)^2 \int_{\mathbf{r}} |\mathbf{r}|^2 \langle \rho(\mathbf{r}) \rangle}$$

$$\rho(\mathbf{r}_1, \mathbf{r}_2) = \langle \delta \rho(\mathbf{r}_1) \delta \rho(\mathbf{r}_2) \rangle = \langle \rho(\mathbf{r}_1) \rho(\mathbf{r}_2) \rangle - \langle \rho(\mathbf{r}_1) \rangle \langle \rho(\mathbf{r}_2) \rangle$$

$$\rho(\mathbf{r}_1, \mathbf{r}_2, \mathbf{r}_3) = \langle \delta \rho(\mathbf{r}_1) \delta \rho(\mathbf{r}_2) \delta \rho(\mathbf{r}_3) \rangle$$

# Imaging shapes of atomic nuclei in high-energy nuclear collisions

Collision geometry depends on the orientations: Head-on collisions have two extremes body-body or tip-tip collisions

Body-body: large-eccentricity large-size

$$v_2 \nearrow \quad p_T \searrow$$

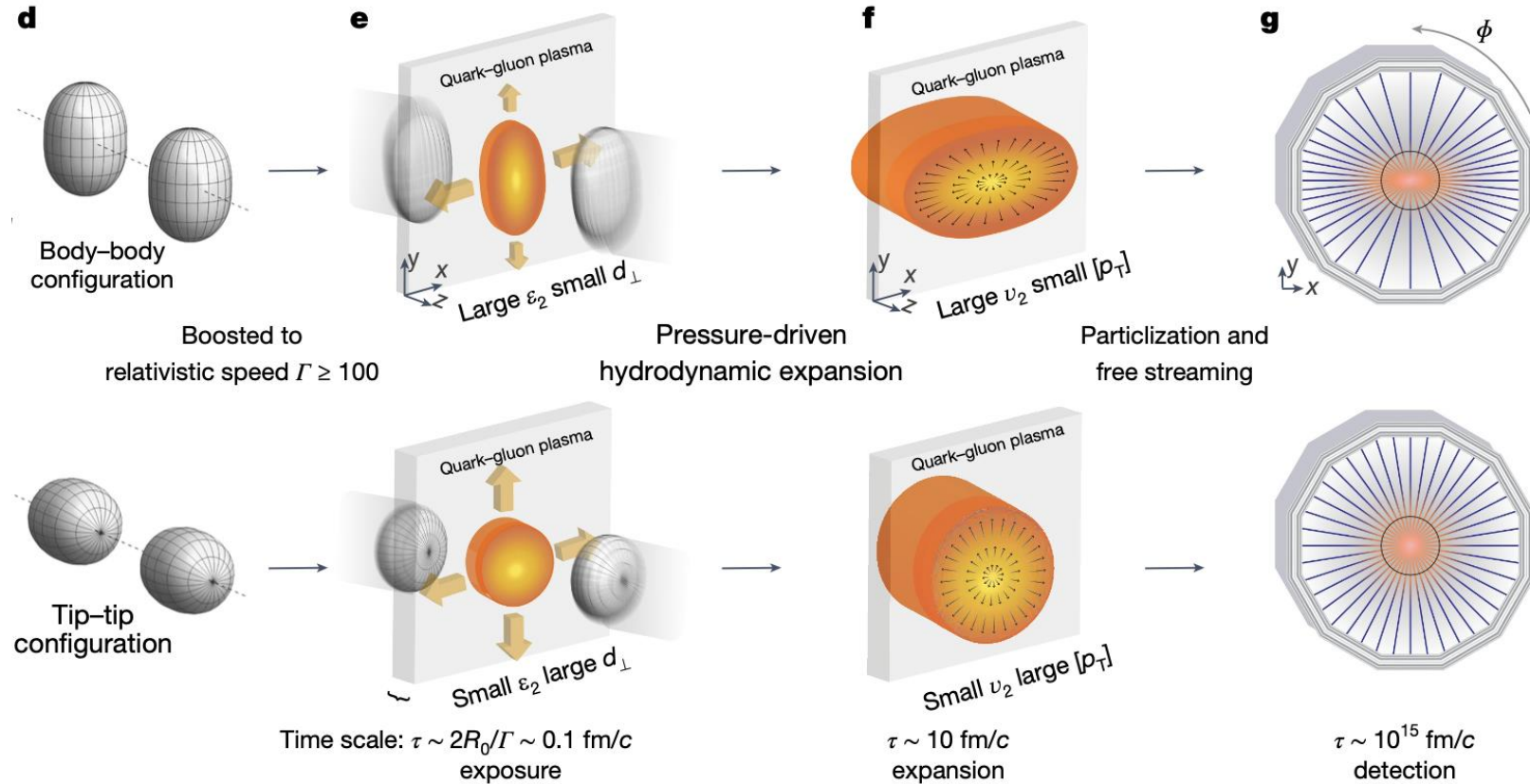
Tip-tip : small-eccentricity small-size

$$v_2 \searrow \quad p_T \nearrow$$

$$\langle v_2^2 \rangle = a_1 + b_1 \beta_2^2,$$

$$\langle (\delta p_T)^2 \rangle = a_2 + b_2 \beta_2^2,$$

$$\langle v_2^2 \delta p_T \rangle = a_3 - b_3 \beta_2^3 \cos(3\gamma).$$



Deformation enhances the fluctuations of  $v_2$  and  $[p_T]$ . Also leads to anticorrelation between  $v_2$  and  $[p_T]$ .

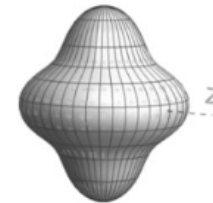
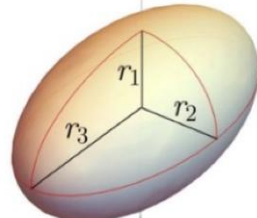
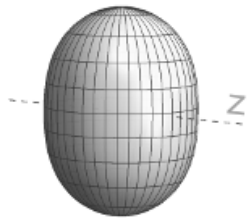
Shape-frozen like snapshot in nuclear crossing ( $10^{-25}s \ll$  rotational time scale  $10^{-21}s$ )

probe entire mass distribution in the intrinsic frame via multi-point correlations

## Nuclear structure in heavy $^{238}\text{U}$ and $^{129}\text{Xe}$ nuclei

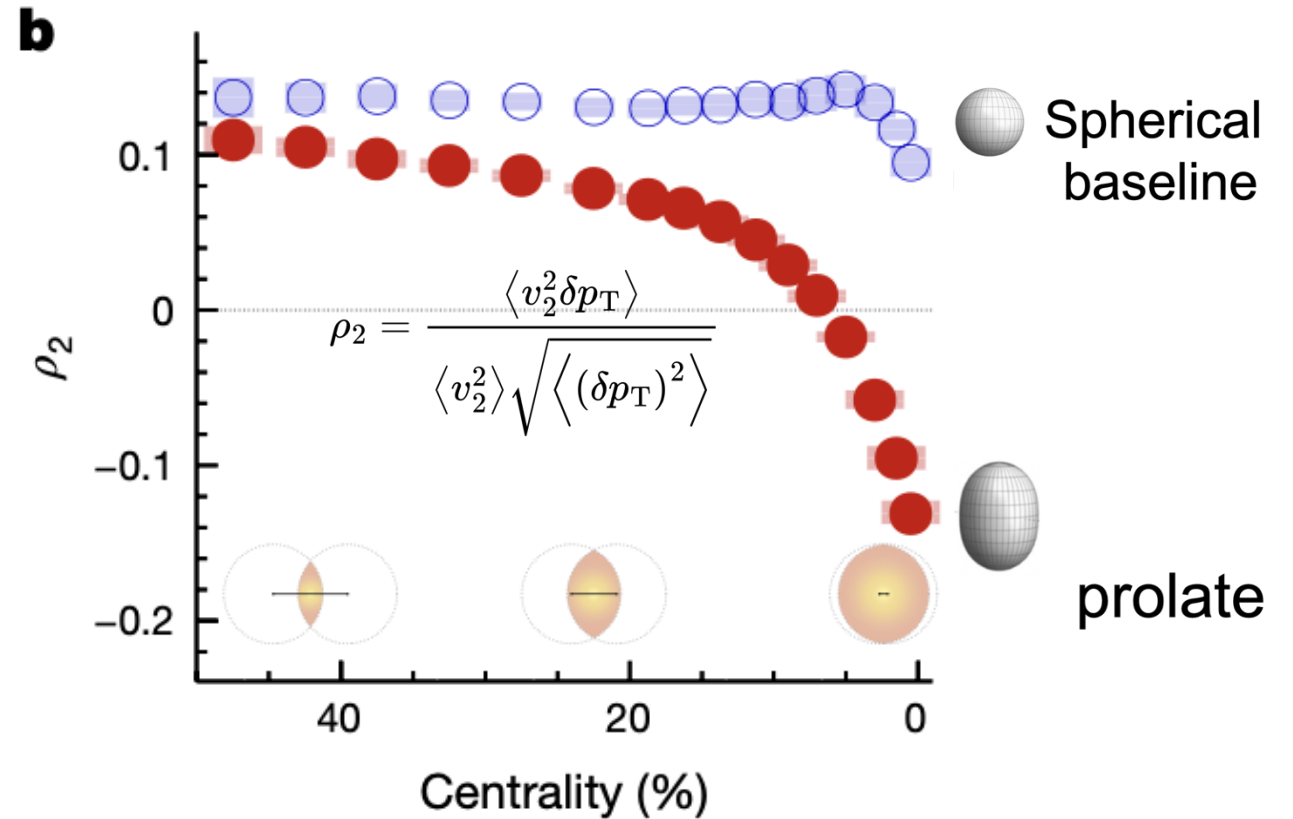
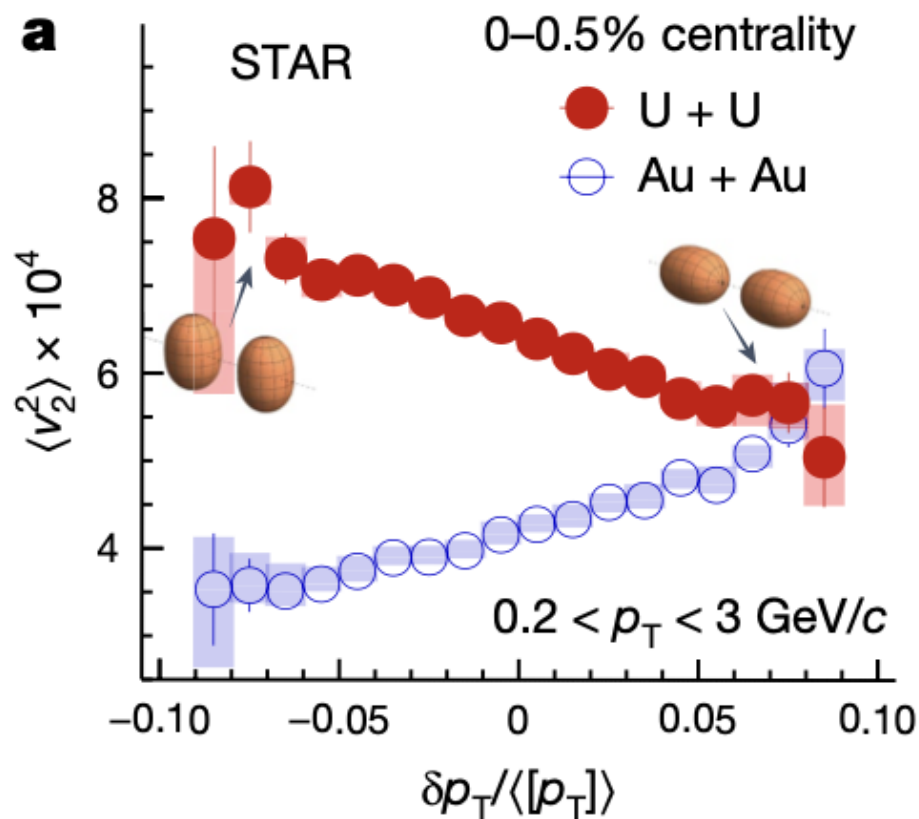
$$\rho(r, \theta, \phi) = \frac{\rho_0}{1 + e^{(r-R(\theta, \phi))/a_0}}$$

$$R(\theta, \phi) = R_0(1 + \beta_2[\cos \gamma Y_{2,0}(\theta, \phi) + \sin \gamma Y_{2,2}(\theta, \phi)] + \beta_3 Y_{3,0}(\theta, \phi) + \beta_4 Y_{4,0}(\theta, \phi))$$



# Impact of quadrupole deformation

Seen directly by comparing  $^{238}\text{U}+^{238}\text{U}$  with near-spherical  $^{197}\text{Au}+^{197}\text{Au}$



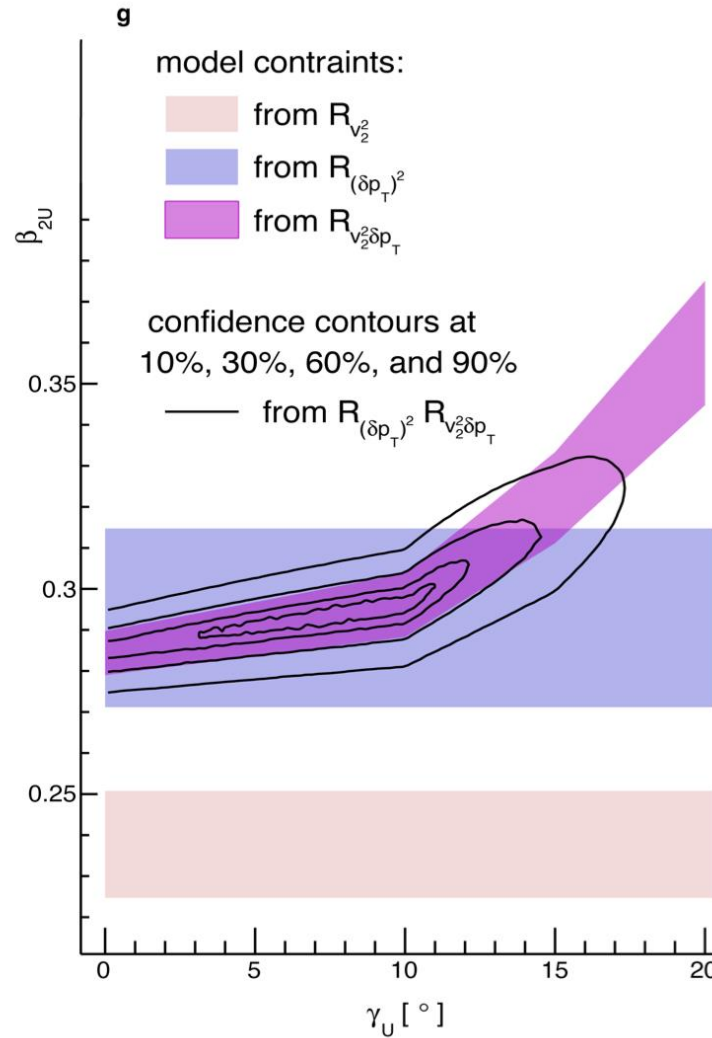
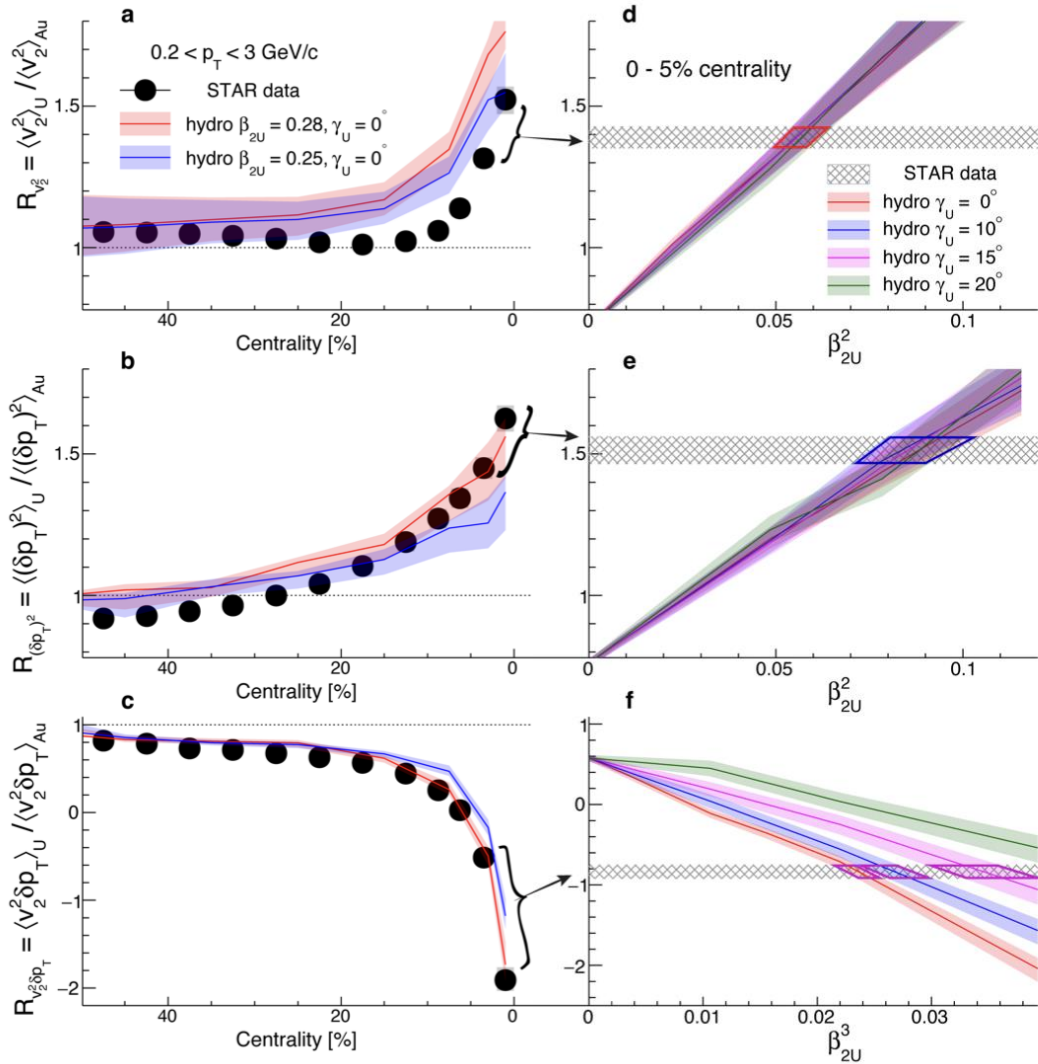
Nature, 635, 67-72 (2024)

<https://doi.org/10.1038/s41586-024-08097-2>

Near-spherical  $\rightarrow$  flat  $\rho_2$  vs centrality

Strongly prolate  $\rightarrow$  decreasing  $\rho_2$  vs centrality

# Extracting shape of $^{238}\text{U}$ : quadrupole deformation and triaxiality



Achieves a better description of ratios in UCC region

Relation confirmed

$$\langle v_2^2 \rangle = a_1 + b_1 \beta_2^2$$

$$\langle (\delta p_T)^2 \rangle = a_2 + b_2 \beta_2^2$$

$$\langle v_2^2 \delta p_T \rangle = a_3 - b_3 \beta_2^3 \cos(3\gamma)$$

Constraints on  $\beta_2$  and  $\gamma$  of  $^{238}\text{U}$  simultaneously with data-hydro-comparison

$$\beta_{2U} = 0.297 \pm 0.015$$

$$\gamma_U = 8.5^\circ \pm 4.8^\circ$$

But we cannot distinguish between rigid triaxiality and triaxial fluctuations  
 This can be done using six-particle correlations:  $v_2\{6\}$ ,  $\langle v_2^4 \delta p_T^2 \rangle$ .

A large deformation with a slight deviation from axial symmetry in the nuclear ground-state

**nature** article metrics

Article metrics | Last updated: Fri, 15 Nov 2024 16:06:26 Z

## Imaging shapes of atomic nuclei in high-energy nuclear collisions

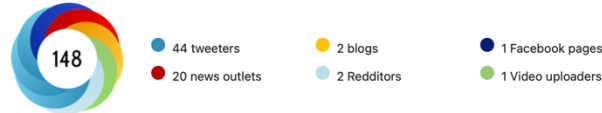
### Access & Citations

39k	0	1
Article Accesses	Web of Science	CrossRef

Citation counts are provided from Web of Science and CrossRef. The counts may vary by service, and are reliant on the availability of their data. Counts will update daily once available.

<https://www.nature.com/articles/s41586-024-08097-2>

### Online attention



This article is in the 99<sup>th</sup> percentile (ranked 1,639<sup>th</sup>) of the 156,500 tracked articles of a similar age in all journals and the 77<sup>th</sup> percentile (ranked 160<sup>th</sup>) of the 699 tracked articles of a similar age in *Nature*

View more on [Altmetric](#)

**nature**

Explore content | About the journal | Publish with us | Subscribe

[nature](#) > [news & views](#) > article

<https://www.nature.com/articles/d41586-024-03466-3>

NEWS AND VIEWS | 06 November 2024

## Rare snapshots of a kiwi-shaped atomic nucleus

Smashing uranium-238 ions together proves to be a reliable way of imaging their nuclei. High-energy collision experiments reveal nuclear shapes that are strongly elongated and have no symmetry around their longest axis.

By [Magda Zielińska](#) & [Paul E. Garrett](#)

**Brookhaven National Laboratory**

Newsroom Media & Communications Office

<https://www.bnl.gov/newsroom/news.php?a=122119>

Newsroom | Photos | Videos | Fact Sheets | Lab History | News Categories

Contact: [Karen McNulty Walsh](#), (631) 344-8350, or [Peter Genzer](#), (631) 344-3174

## Imaging Nuclear Shapes by Smashing them to Smitheren

Scientists use high-energy heavy ion collisions as a new tool to reveal subtleties of nuclear structure in many areas of physics

November 6, 2024



**nature**

Explore content | About the journal | Publish with us | Subscribe

[nature](#) > [news](#) > article

<https://www.nature.com/articles/d41586-024-03633-6>

NEWS | 06 November 2024

## Smashing atomic nuclei together reveals their elusive shapes

A method to take snapshots of exploding nuclei could hold clues about the fundamental properties of gold, uranium and other elements.

By [Elizabeth Gibney](#)

**nature**

Explore content | About the journal | Publish with us | Subscribe

[nature](#) > [nature podcast](#) > article

<https://www.nature.com/articles/d41586-024-03646-1>

NATURE PODCAST | 06 November 2024

## Surprise finding reveals mitochondrial 'energy factories' come in two different types

Mitochondria divide to share the load when nutrients are scarce – plus, how smashing atomic nuclei together helps identify their shapes.

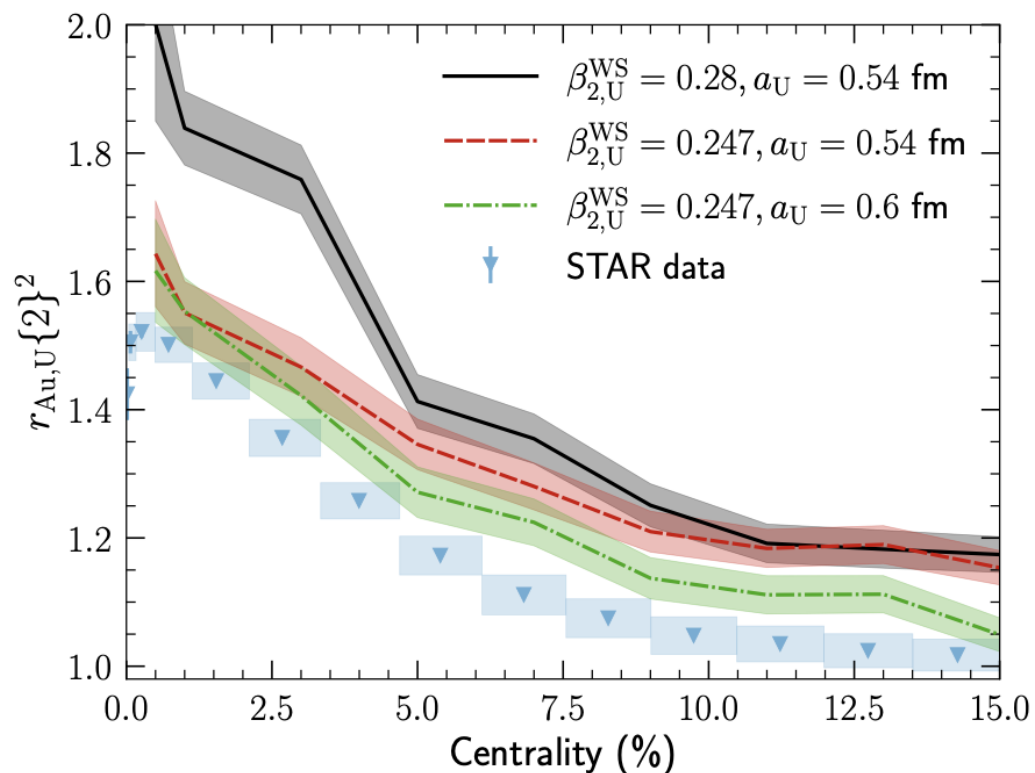
By [Benjamin Thompson](#) & [Emily Bates](#)

中国物理学会 中国科学院物理研究所 主办

low energy estimate  $\beta_{2\text{U}} = 0.287 \pm 0.009$

Value could be smaller due to possible  $\beta_4$ .

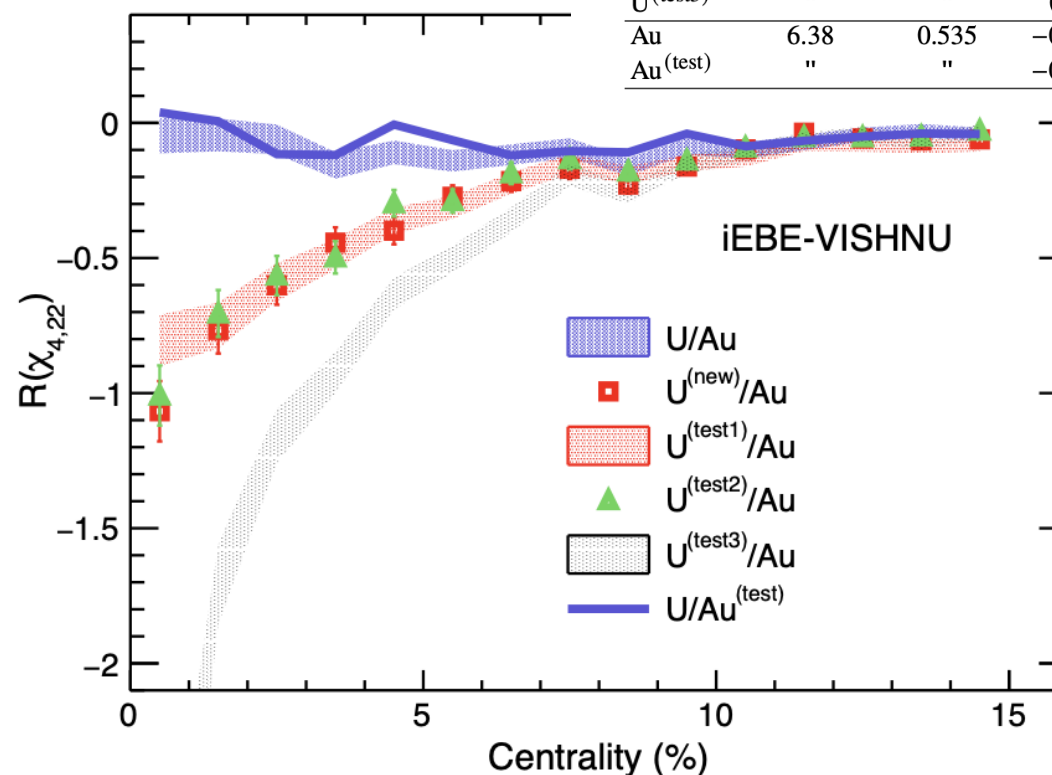
$$\beta_{2\text{U}} \sim 0.25 - 0.26$$



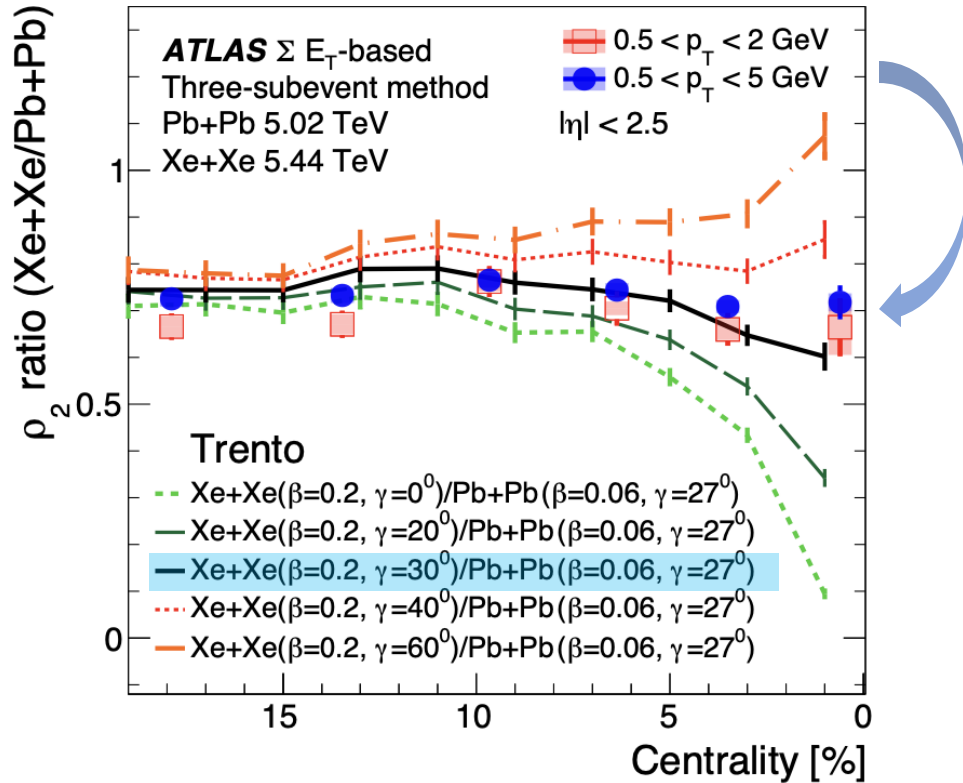
High-order deformation is hard to measure at low energy

TABLE I. WS parameters for  $^{238}\text{U}$  and  $^{197}\text{Au}$  used in this Letter.

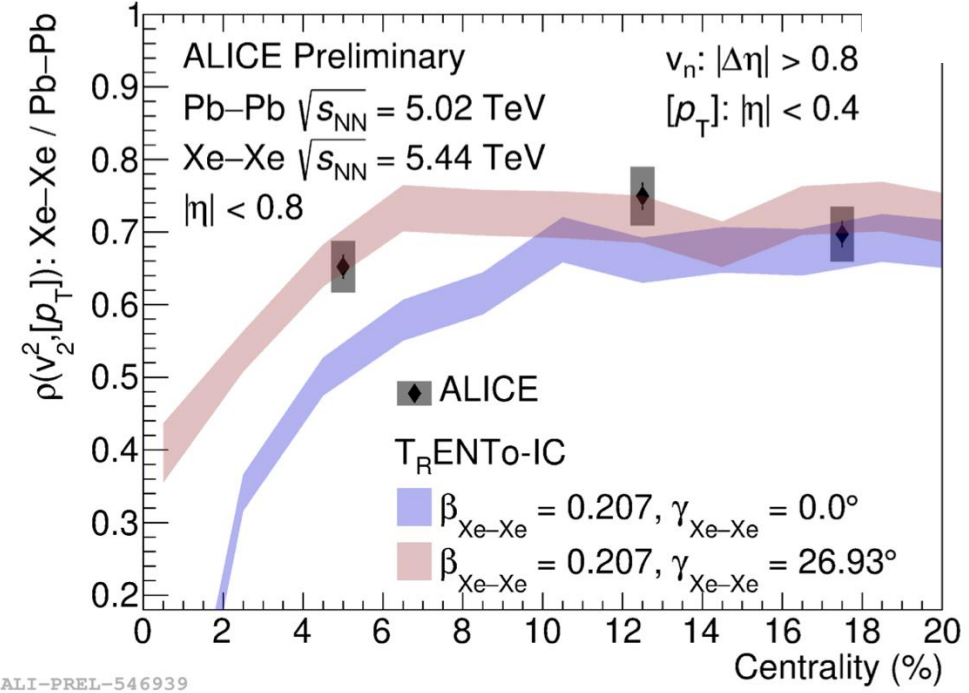
	$R_0$ (fm)	$a$ (fm)	$\beta_2$	$\beta_4$
U	6.87	0.556	0.286	0.000
U <sup>(new)</sup>	6.90	0.538	0.259	0.100
U <sup>(test1)</sup>	6.87	0.556	0.286	0.100
U <sup>(test2)</sup>	"	"	0.232	0.100
U <sup>(test3)</sup>	"	"	0.286	0.200
Au	6.38	0.535	-0.131	-0.031
Au <sup>(test)</sup>	"	"	-0.160	"



ATLAS, PRC 107, 054910(2023)



ALICE, PLB 834, 137393(2022)  
 Emil Gorm Nielsen, ALICE, QM2023  
 ALICE, 2409.04343



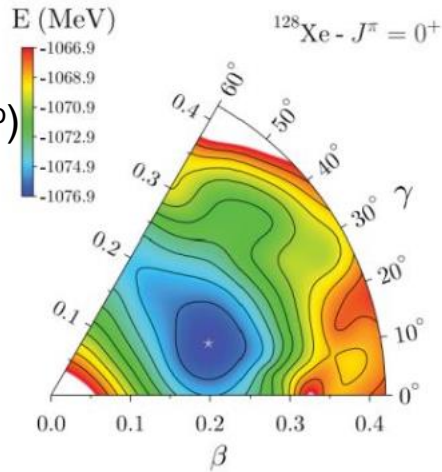
- The medium effect was mostly canceled.
- Study the triaxial shape of  $^{129}\text{Xe}$  nuclei  
 Triaxiality fluctuation could wash out the difference between prolate and oblate.

- ALICE data suggests a triaxial structure of  $^{129}\text{Xe}$

## Consistency between ATLAS and ALICE

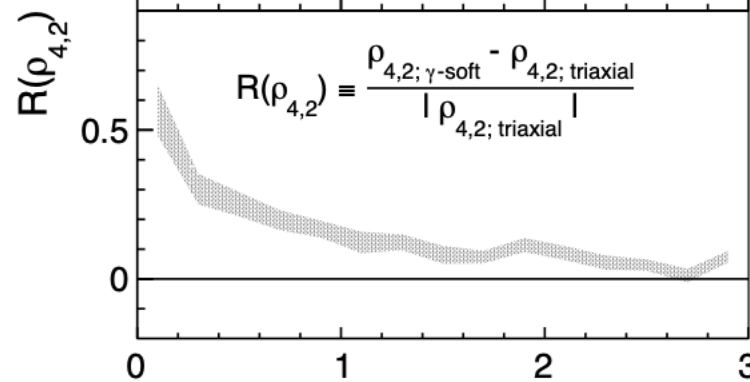
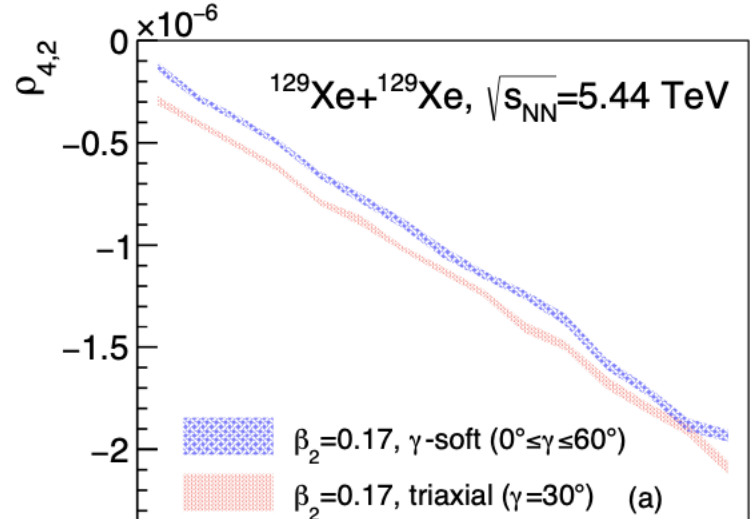
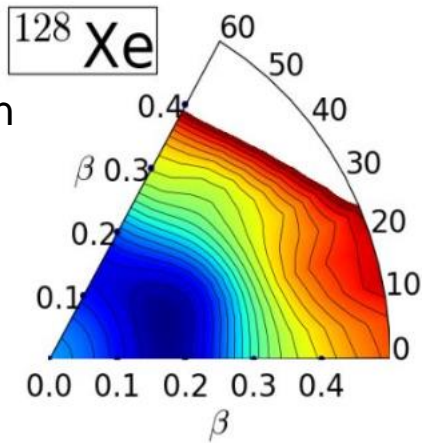
# Probe $\gamma$ -rigid or $\gamma$ -soft of the $^{129}\text{Xe}$

Rigid triaxial deformation ( $\gamma=30^\circ$ )  
Bally et. al.  
EPJA58 (2022) 9, 187

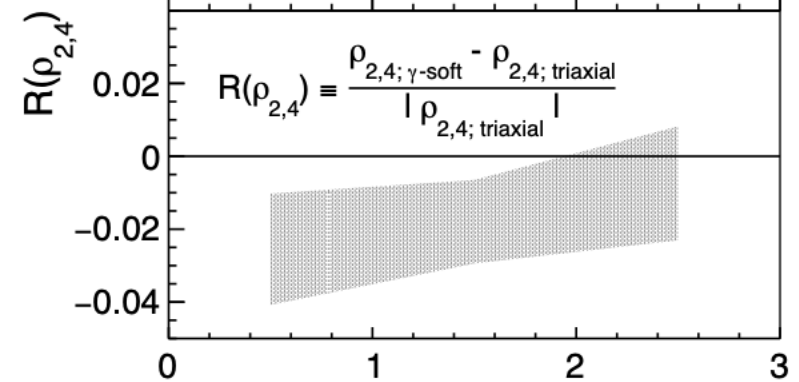
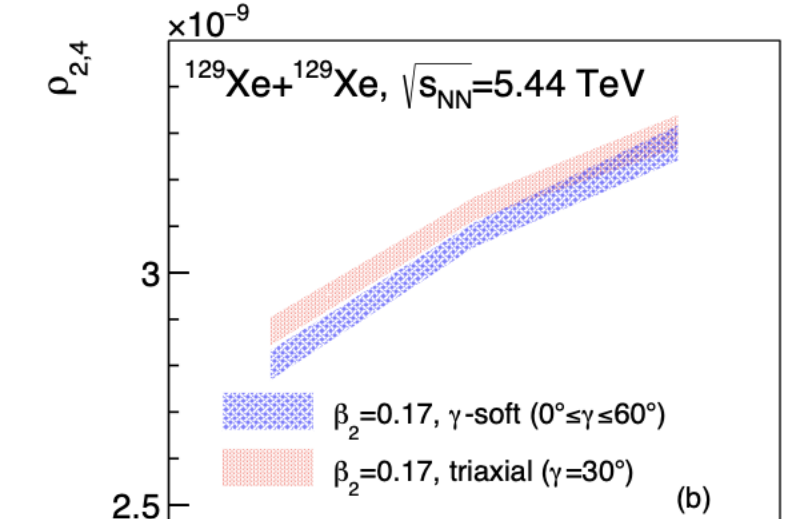


$\gamma$ -soft (flat distribution in  $0 \leq \gamma \leq 60^\circ$ )

Z. P. Li, et. al. PRC81, 034316 (2010)



$$\rho_{4,2} \equiv \left( \frac{\langle \varepsilon_2^4 \delta d_\perp^2 \rangle}{\langle \varepsilon_2^4 \rangle \langle d_\perp \rangle^2} \right)_c \quad \text{Centrality}(\%)$$

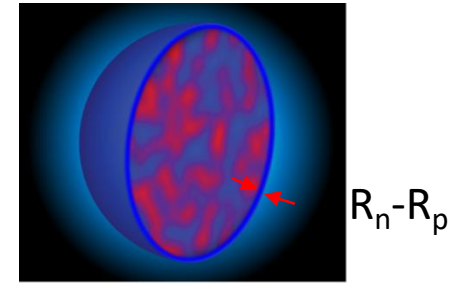


$$\rho_{2,4} \equiv \left( \frac{\langle \varepsilon_2^2 \delta d_\perp^4 \rangle}{\langle \varepsilon_2^2 \rangle \langle d_\perp \rangle^4} \right)_c \quad \text{Centrality}(\%)$$

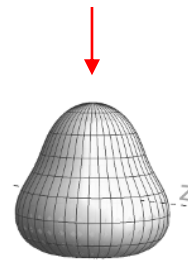
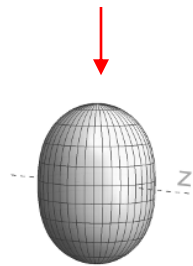
The  $\gamma$ -soft deformation of  $^{129}\text{Xe}$  lead to a clear enhancement of 6-particle correlations  $\rho_{4,2}$  in ultra-central Xe+Xe

## Nuclear structure of intermediate isobaric $^{96}\text{Ru}$ and $^{96}\text{Zr}$ nuclei

$$\rho(r, \theta, \phi) = \frac{\rho_0}{1 + e^{(r-R(\theta, \phi))/a_0}} \longrightarrow$$



$$R(\theta, \phi) = R_0(1 + \beta_2[\cos \gamma Y_{2,0}(\theta, \phi) + \sin \gamma Y_{2,2}(\theta, \phi)] + \beta_3 Y_{3,0}(\theta, \phi))$$



## US Long Range Plan 2023

### Sidebar 6.2 Radioisotope harvesting at FRIB for fundamental physics

The Facility for Rare Isotope Beams (FRIB) will yield the discovery of new, exotic isotopes and the measurement of reaction rates for nuclear astrophysics, and will produce radioactive isotopes that can be used for a broad range of applications, including medicine, biology, and fundamental physics.

#### Converting waste to wealth

Radioisotopes at FRIB are produced via fragmentation when accelerated ion beams interact with a thin target. Several isotopes, including those previously unobserved, across the entire periodic table will be produced in practical quantities for the first time in the water beam dump at the FRIB accelerator. The Isotope Harvesting Project provides a new opportunity to collect these isotopes, greatly enhancing their yield and real-time availability to enable a broad spectrum of research across multiple scientific disciplines. Isotopes will be extracted from the beam dump and chemically purified using radiochemistry techniques in a process called harvesting. Harvesting operates commensally, therefore providing additional opportunities for science.

#### Pear-shaped nuclei enable new-physics searches

With uranium-238 ion beams, these methods can produce heavy, pear-shaped nuclei that can be used to search for violations of fundamental symmetries that would signal new forces in nature. For example, a nonzero permanent electric dipole moment (EDM) would break parity and time-reversal symmetries. Figure 1 shows a pear-shaped nucleus spinning under applied electric and magnetic fields. Its magnetic dipole moment (MDM) is nonzero, and if its EDM is also nonzero, then its spin-precession rate changes if the direction of time is reversed. Heavy, pear-shaped nuclei can greatly amplify the sensitivity to a nonzero EDM and complement neutron EDM studies. Pear-shaped isotopes such as radium-225 and protactinium-229 will be produced in abundance at FRIB, and their EDM effects can be further enhanced by using them to form polar molecules, which can then be probed using cutting-edge laser techniques. The unique sensitivity of these experiments opens otherwise inaccessible windows on new physics.

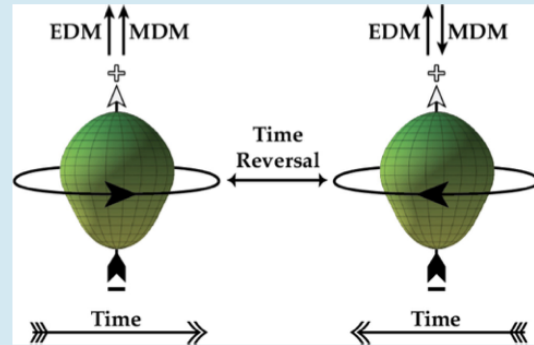
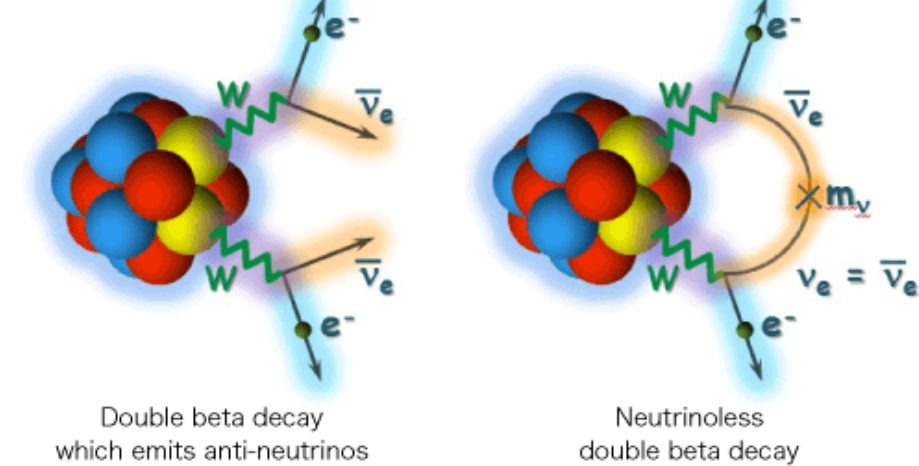


Figure 1. A pear-shaped nucleus spins counterclockwise or clockwise, depending on the direction of time. [S47]

## Hunt for the no neutrinos

### [Double beta decay]



Isotope	$T_{1/2}^{0\nu} (\times 10^{25} \text{ y})$	$\langle m_{\beta\beta} \rangle (\text{eV})$	Experiment	Reference
$^{48}\text{Ca}$	$> 5.8 \times 10^{-3}$	$< 3.5 - 22$	ELEGANT-IV	(157)
$^{76}\text{Ge}$	$> 8.0$	$< 0.12 - 0.26$	GERDA	(158)
	$> 1.9$	$< 0.24 - 0.52$	MAJORANA DEMONSTRATOR	(159)
$^{82}\text{Se}$	$> 3.6 \times 10^{-2}$	$< 0.89 - 2.43$	NEMO-3	(160)
$^{96}\text{Zr}$	$> 9.2 \times 10^{-4}$	$< 7.2 - 19.5$	NEMO-3	(161)
$^{100}\text{Mo}$	$> 1.1 \times 10^{-1}$	$< 0.33 - 0.62$	NEMO-3	(162)
$^{116}\text{Cd}$	$> 1.0 \times 10^{-2}$	$< 1.4 - 2.5$	NEMO-3	(163)
$^{128}\text{Te}$	$> 1.1 \times 10^{-2}$	—	—	(164)
$^{130}\text{Te}$	$> 1.5$	$< 0.11 - 0.52$	CUORE	(124)
$^{136}\text{Xe}$	$> 10.7$	$< 0.061 - 0.165$	KamLAND-Zen	(165)
	$> 1.8$	$< 0.15 - 0.40$	EXO-200	(166)
$^{150}\text{Nd}$	$> 2.0 \times 10^{-3}$	$< 1.6 - 5.3$	NEMO-3	(167)

$^{96}\text{Zr}$  with high-case rate, strong neutrino mass limiting ability

EDMs are very small and difficult to measure.

Higher sensitivity via Schiff nuclear moments in heavy nuclei

-> Octupole deformation enhancements

$$T_{1/2}^{0\nu} = \left( G |\mathcal{M}|^2 \langle m_{\beta\beta} \rangle^2 \right)^{-1} \simeq 10^{27-28} \left( \frac{0.01\text{eV}}{\langle m_{\beta\beta} \rangle} \right)^2 \text{ y}$$

Nuclear matrix element

# Unique isobar $^{96}\text{Ru}$ and $^{96}\text{Zr}$ Collisions

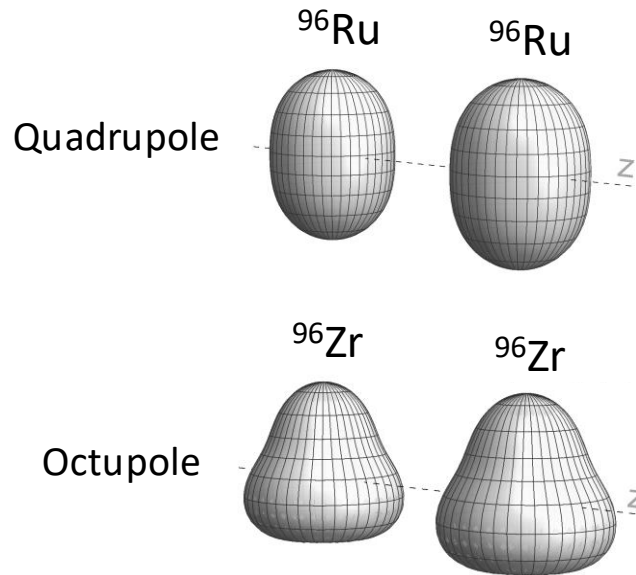
$^{96}\text{Ru}+^{96}\text{Ru}$  and  $^{96}\text{Zr}+^{96}\text{Zr}$  at  $\sqrt{s_{NN}} = 200$  GeV

- A key question for any HI observable  $\mathcal{O}$ :
- Expectation:

$$\frac{\mathcal{O}_{^{96}\text{Ru}} + \mathcal{O}_{^{96}\text{Ru}}}{\mathcal{O}_{^{96}\text{Zr}} + \mathcal{O}_{^{96}\text{Zr}}} \stackrel{?}{=} 1$$

Deviation from 1 could have an origin in the nuclear structure, which impacts the initial state and then survives to the final state.

$$\mathcal{O} \approx b_0 + b_1\beta_2^2 + b_2\beta_3^2 + b_3(R_0 - R_{0,\text{ref}}) + b_4(a - a_{\text{ref}})$$



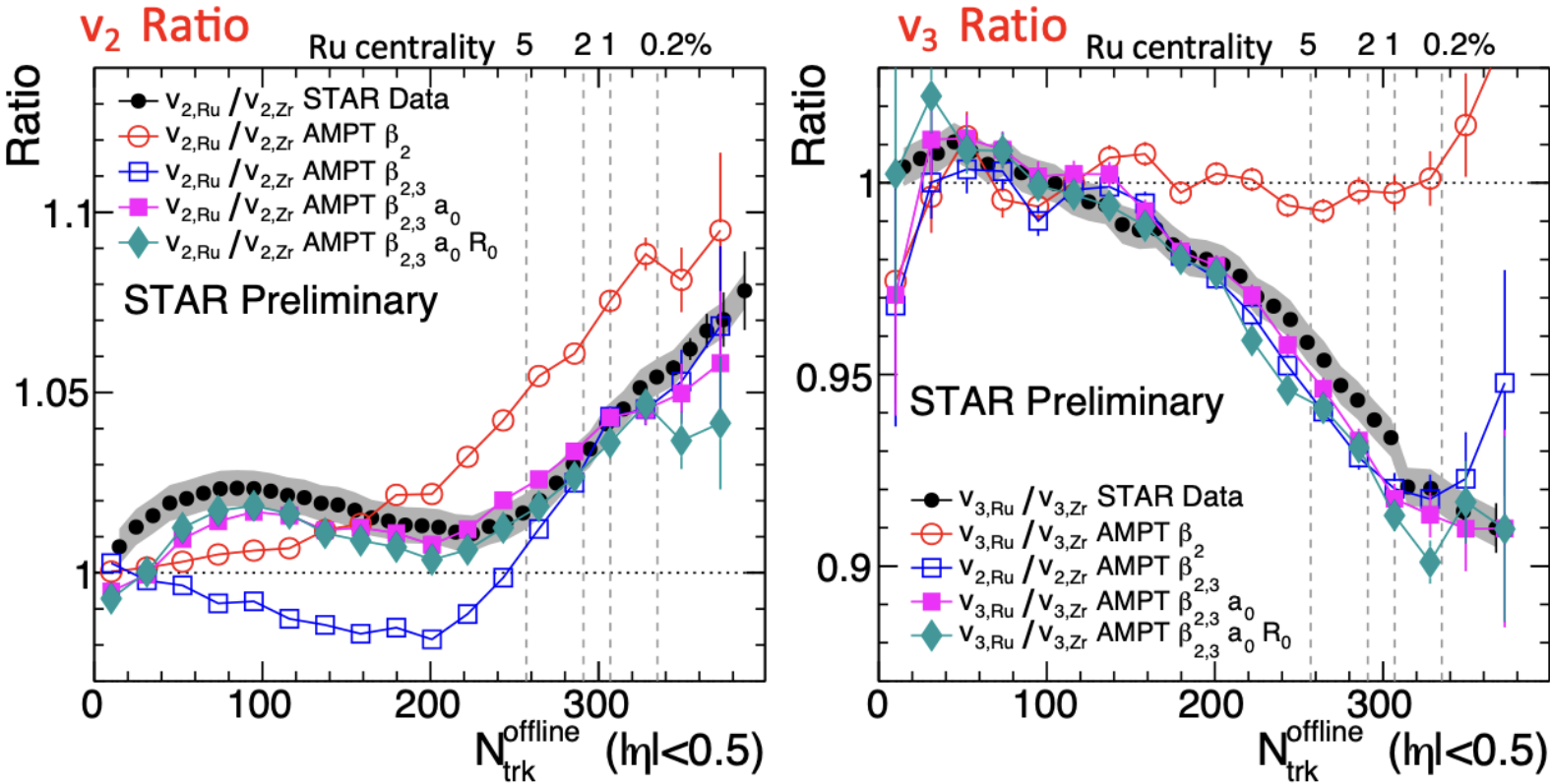
$$R_{\mathcal{O}} \equiv \frac{\mathcal{O}_{\text{Ru}}}{\mathcal{O}_{\text{Zr}}} \approx 1 + c_1\Delta\beta_2^2 + c_2\Delta\beta_3^2 + c_3\Delta R_0 + c_4\Delta a$$

Probe structure differences

Low energy measurement

	$\beta_2$	$E_{2^+_1}$ (MeV)	$\beta_3$	$E_{3^-_1}$ (MeV)
$^{96}\text{Ru}$	0.154	0.83	-	3.08
$^{96}\text{Zr}$	0.062	1.75	0.202,0.235,0.27	1.90

Evidence of static octupole moments at low energies is rather sparse.



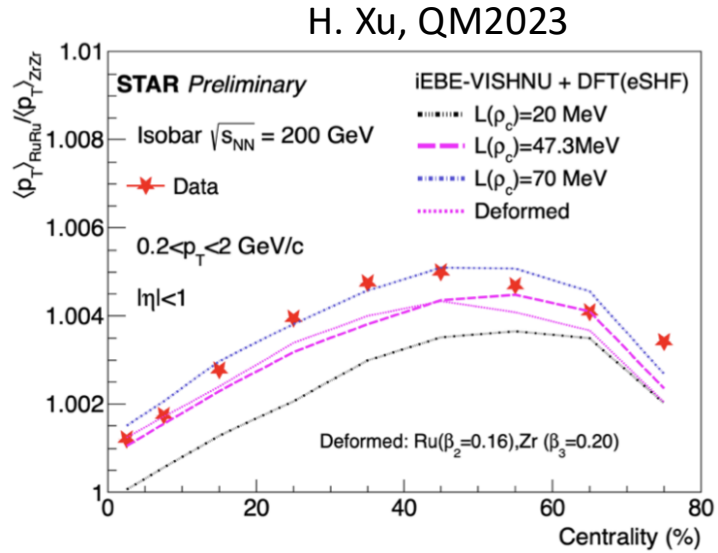
- $\beta_{2Ru} \sim 0.16$  increase  $v_2$ , no influence on  $v_3$  ratio
- $\beta_{3Zr} \sim 0.2$  decrease  $v_2$  in mid-central, decrease  $v_3$  ratio
- $\Delta a_0 = -0.06$  fm increase  $v_2$  mid-central, small impact on  $v_3$
- Radius  $\Delta R_0 = 0.07$  fm only slightly affects  $v_2$  and  $v_3$  ratio.

Species	$\beta_2$	$\beta_3$	$a_0$	$R_0$
Ru	0.162	0	0.46 fm	5.09 fm
Zr	0.06	0.20	0.52 fm	5.02 fm
difference	$\Delta\beta_2^2$	$\Delta\beta_3^2$	$\Delta a_0$	$\Delta R_0$
	0.0226	-0.04	-0.06 fm	0.07 fm

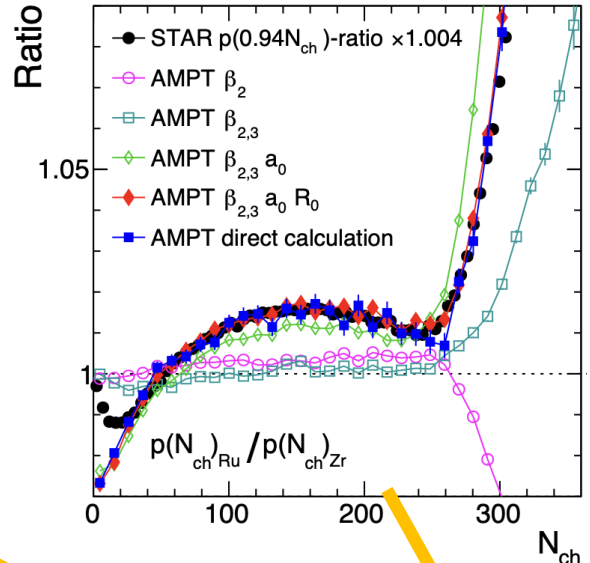
- Direct observation of octupole deformation in  $^{96}\text{Zr}$  nucleus
- Clearly imply the neutron skin difference between  $^{96}\text{Ru}$  and  $^{96}\text{Zr}$
- Simultaneously constrain these parameters using different  $N_{\text{ch}}$  regions

# Imaging the radial structures (neutron skin)

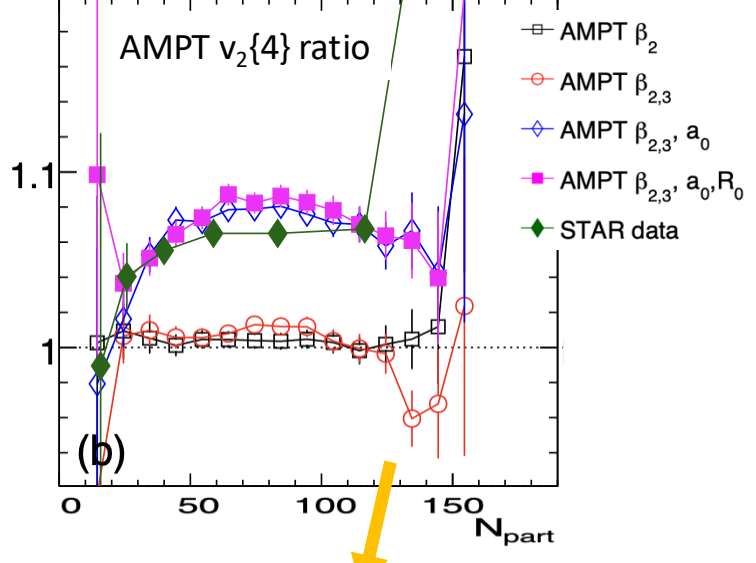
Radial parameters  $R_0$ ,  $a_0$  are properties of one-body distribution  $\rightarrow \langle p_T \rangle, \langle N_{ch} \rangle, v_2^{RP} \sim v_2\{4\}, \sigma_{tot}$



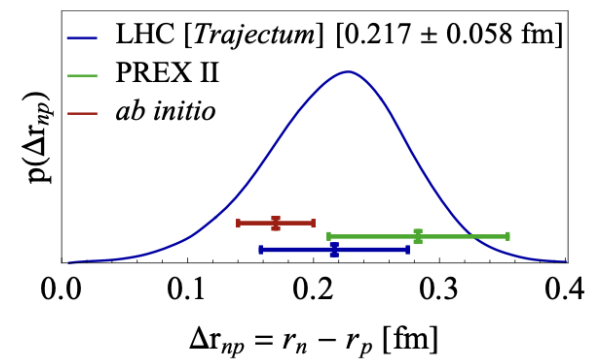
J. Jia, C. Zhang, PRC 107, L02901 (2023)



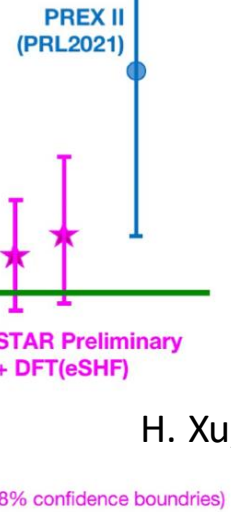
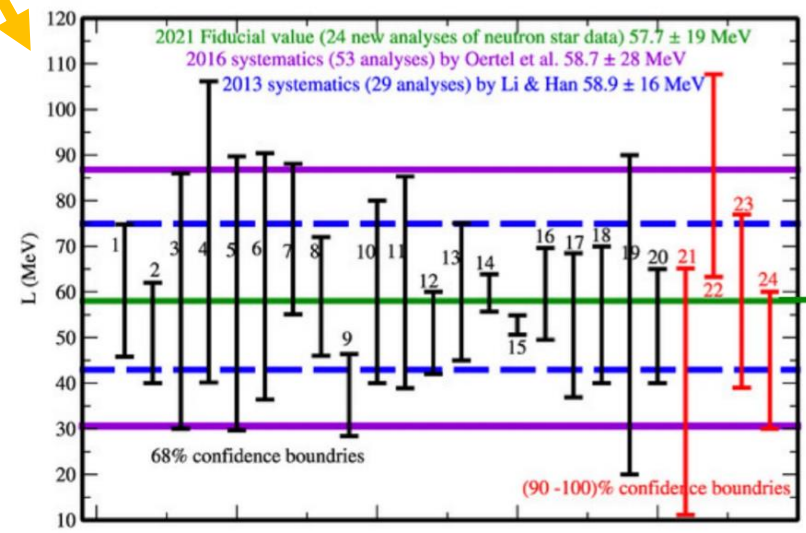
J. Jia, G. Giacalone, C. Zhang, PRL 131, 022301(2023)



B. Li, et.al Universe 7, 182 (2021)



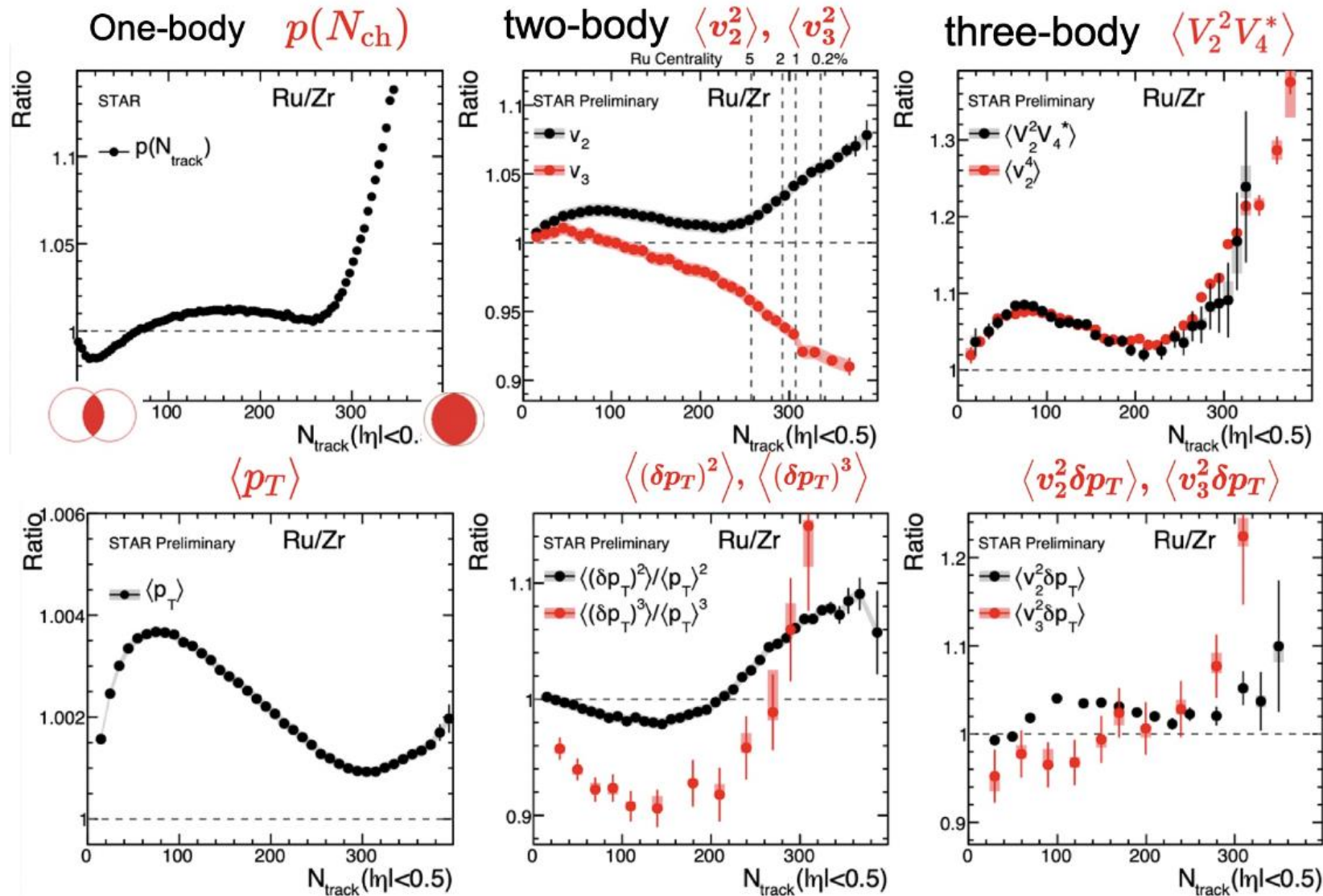
G. Giacalone, G. Nijs, W. Schee, PRL 131, 202302(2023)



H. Xu, QM2023

## Constrain neutron skin and symmetry energy

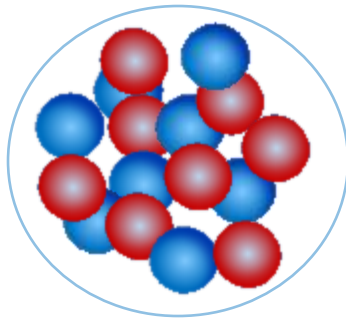
# Nuclear structure influences everywhere



Nuclear structure is inherently part of heavy ion problem

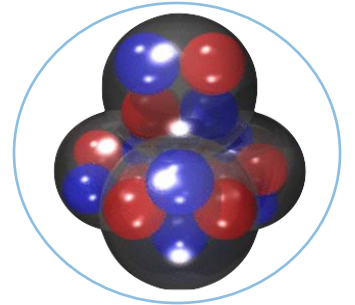
# Benchmarking tomography of many-body correlation in light $^{16}\text{O}$ nucleus

--- from one-body distribution to many-body nucleon correlations



$$\rho(r) \propto \frac{1 + w(r^2/R^2)}{1 + e^{(r-R)/a_0}}$$

→ first-principle ab initio framework



Hideki Yukawa



“for his prediction of the existence of mesons on the basis of theoretical work on nuclear forces”

# Nucleon nucleon correlations in finite quantum many-body systems 24

Possible cluster in ground-state  $^{16}_8\text{O}$  nuclei based on low energy, but **NO** evidence.

**Woods-Saxon: without many-body nuclear correlation**

**Nuclear Lattice Effective Field theory (NLEFT): model with many-nucleon correlation including  $\alpha$  clusters**

Lu et al., PLB797, 134863(2019)

M. Freer et al., RevModPhys90, 035004(2018)

S. Elhatisari et al. Nature 630, 59 (2024)

Calculations from Dean Lee

**Variational auxiliary field diffusion Monte Carlo (VMC):**

MC solution of Schrödinger eq. from the time evolution of trial wave function.

A. Lonardononi et al., PRC97, 044318(2018)

J. Carlson and R. Schiavilla, RevModPhys70, 743(1998)

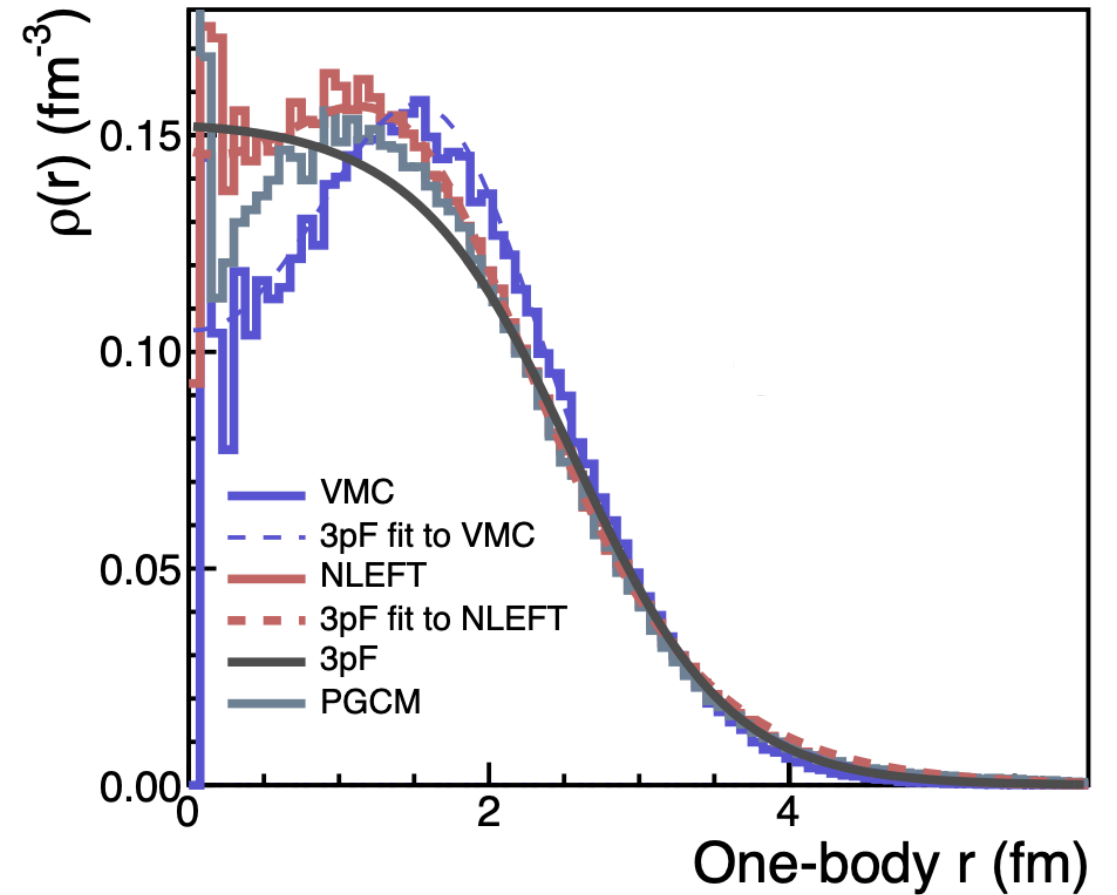
**ab-initio Projected Generator Coordinate Method (PGCM):**

Wave function from variational calculation (as in density functional theory)

Frosini et al., EPJA58, 62(2022); EPJA58, 63(2022);

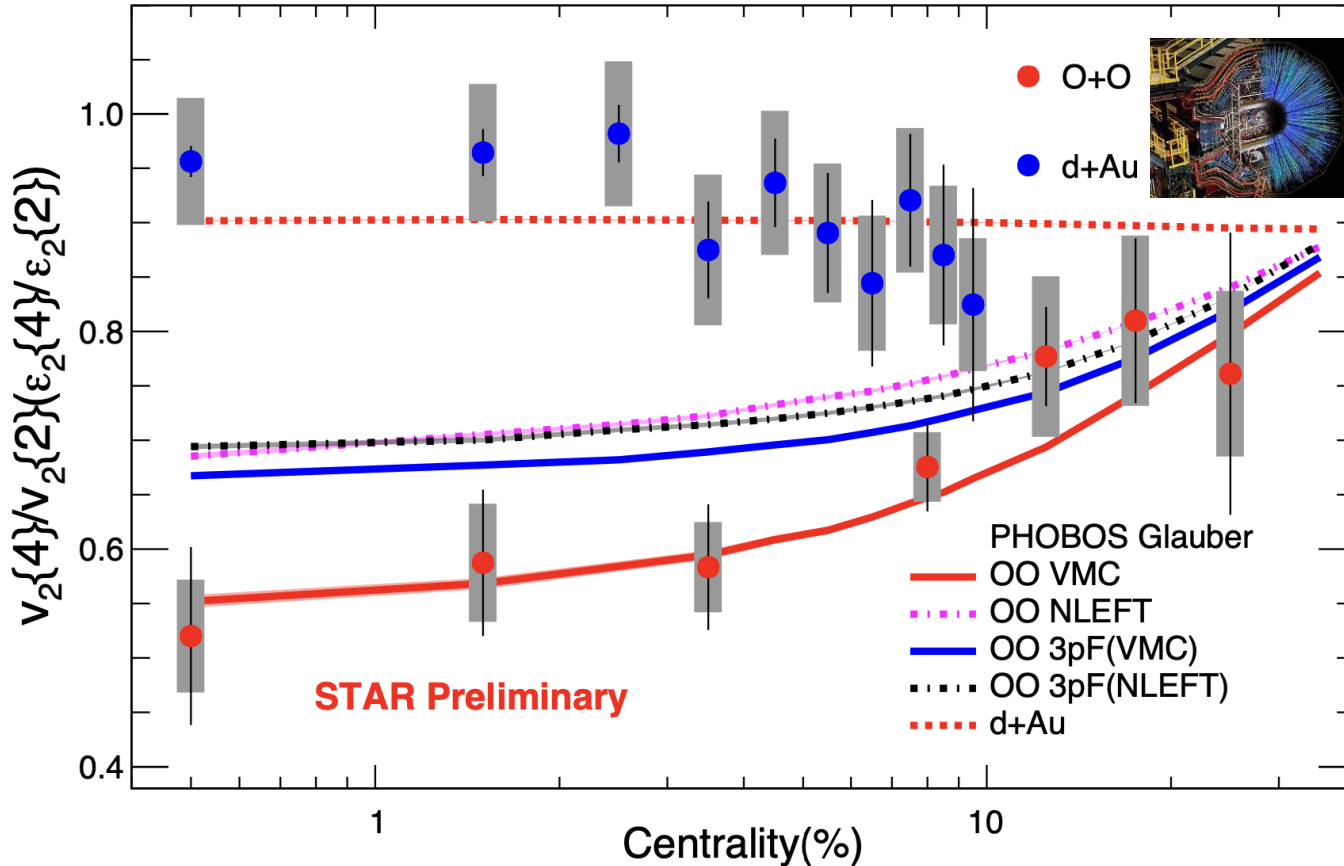
EPJA58, 64(2022)

Calculations from Benjamin Bally



# Geometric tomography of $^{16}\text{O}$ nucleus for the first time in HI

O+O run2021: 600M MB and 250M HM events



$\epsilon_2\{4\} / \epsilon_2\{2\}$  from three models:

1. *WS is away from STAR data.*
2. *VMC and EFT have a visible difference.*

*Can many-nucleon correlations significantly impact the eccentricity fluctuations? YES!*

VMC and EFT theory have visible differences describing the  $v_2\{4\}/v_2\{2\}$ . **The interplay between sub-nucleon fluctuation and many-nucleon correlation.**

STAR, PRL130, 242301(2023)

$$(v_n\{2\})^2 = c_n\{2\} = \langle v_n^2 \rangle$$

$$(v_n\{4\})^4 = -c_n\{4\} = 2\langle v_n^2 \rangle^2 - \langle v_n^4 \rangle$$

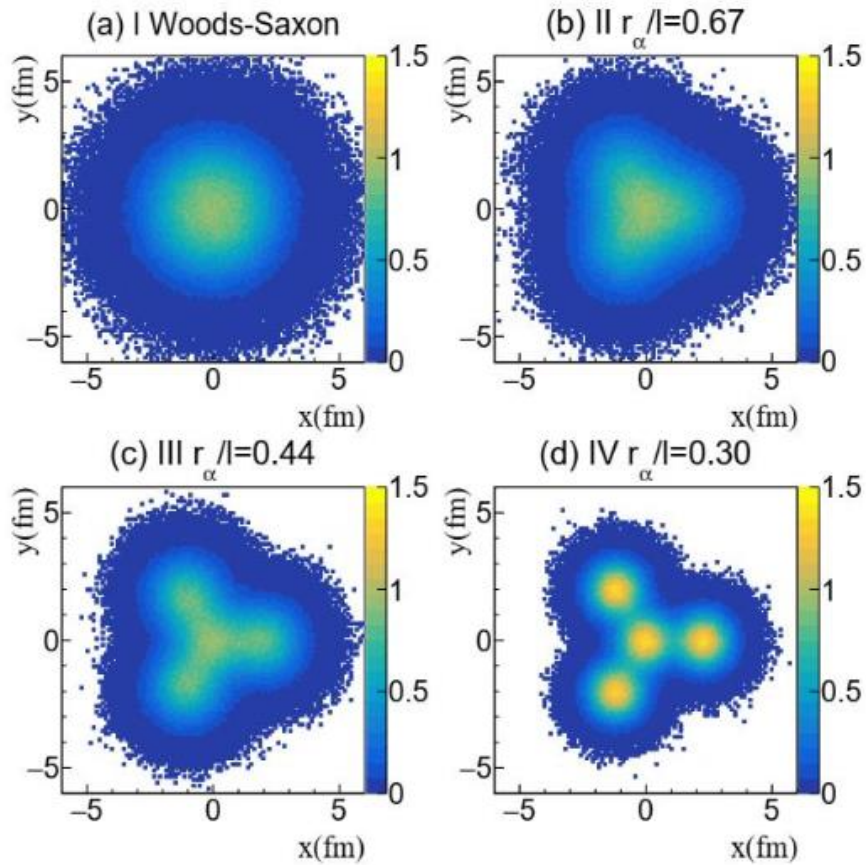
$$\epsilon_2\{2\}^2 = \langle \epsilon_2^2 \rangle$$

$$\epsilon_2\{4\}^4 = 2\langle \epsilon_2^2 \rangle^2 - \langle \epsilon_2^4 \rangle$$

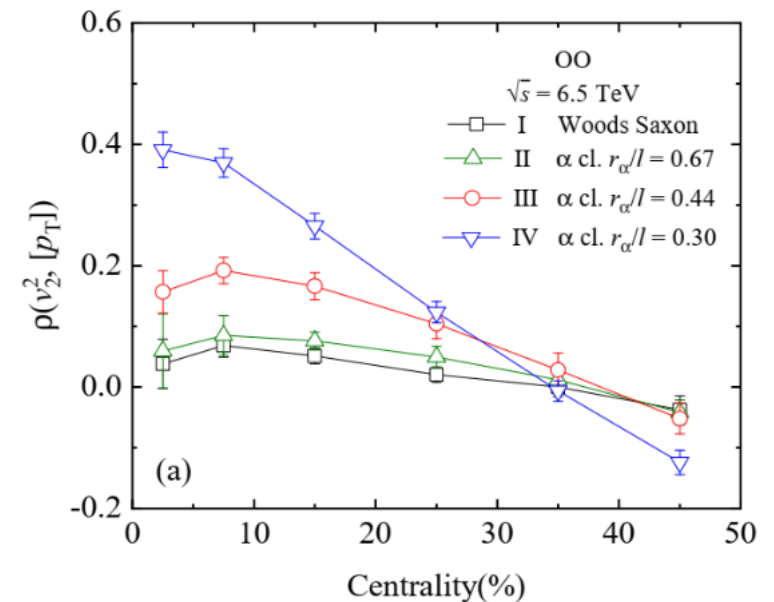
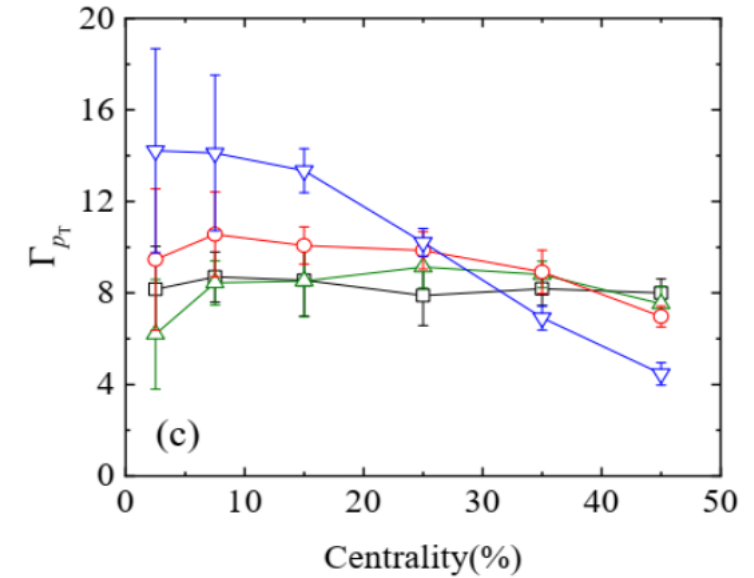
**O+O and p+O at LHC Run2025 possible Ne+Ne collisions?**

Geometric scan elucidates **nuclear tomography** and **strong nuclear force?**

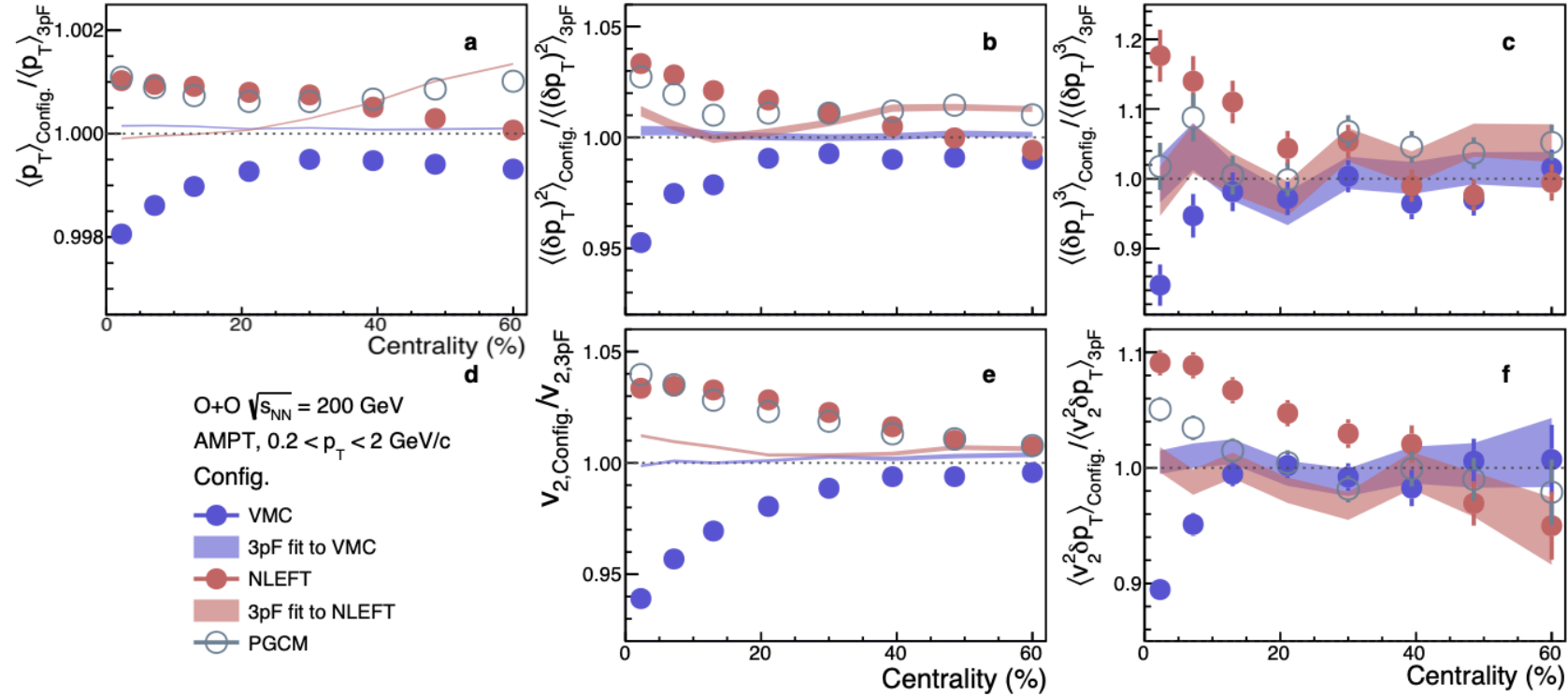
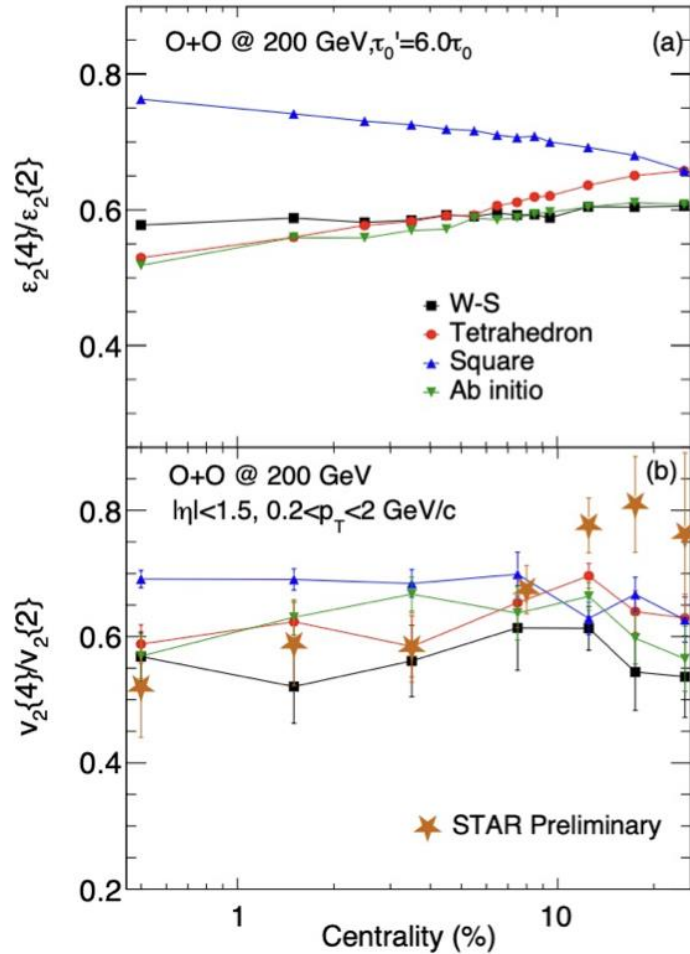
# Searching for signatures of $\alpha$ clusters in different models



$\Gamma$  and  $v_n - p_T$  correlations in  $^{16}\text{O}+^{16}\text{O}$  collisions are sensitive to the compactness of the  $\alpha$  cluster in  $^{16}\text{O}$



# Searching for signatures of $\alpha$ clusters in different models



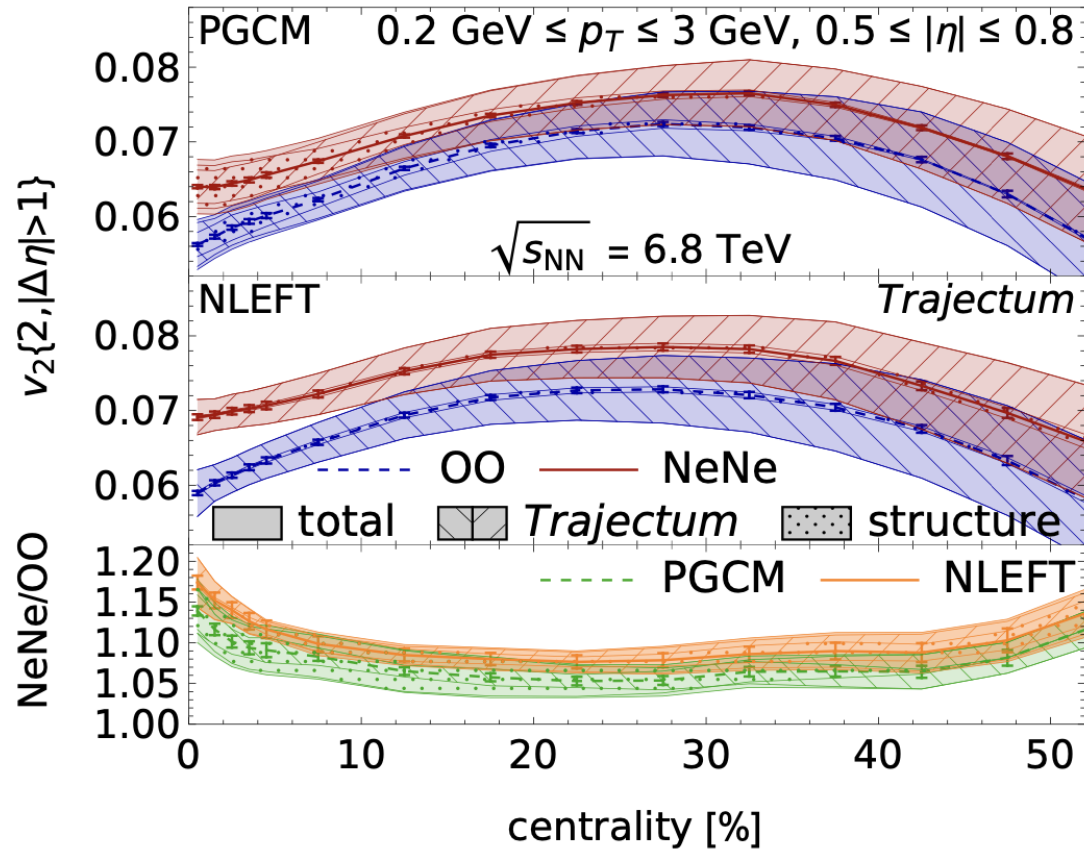
Compared to the STAR on the  $v_2\{4\} / v_2\{2\}$  ratio, the tetrahedron and *ab initio* cases give better descriptions of the STAR data.

Various observables all show sensitivities from different configurations

C. Zhang, J. Chen, G. Giacalone, S. Huang, J. Jia and Y. Ma, 2404.08385

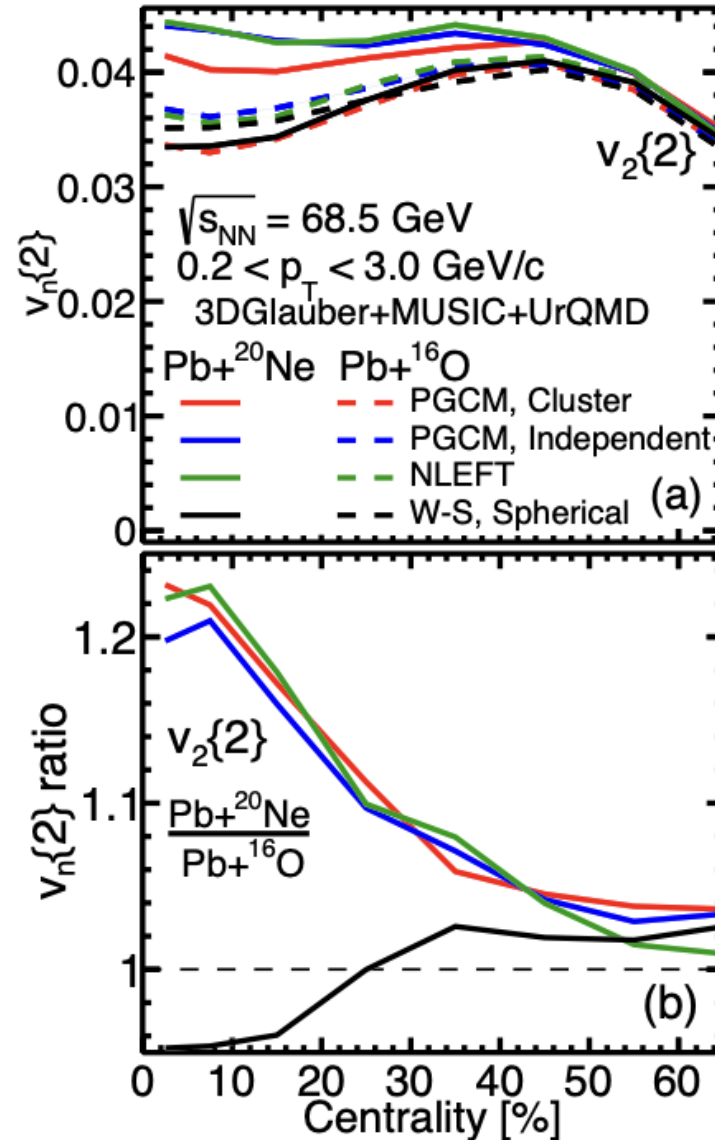
X. Zhao, G. Ma. Y. Zhou, Z. Lin and C. Zhang, 2404.09780

# Searching for signatures of $\alpha$ clusters in different models



a precision test of hydrodynamics in small systems.

NLEFT and PGCM are consistent within uncertainties

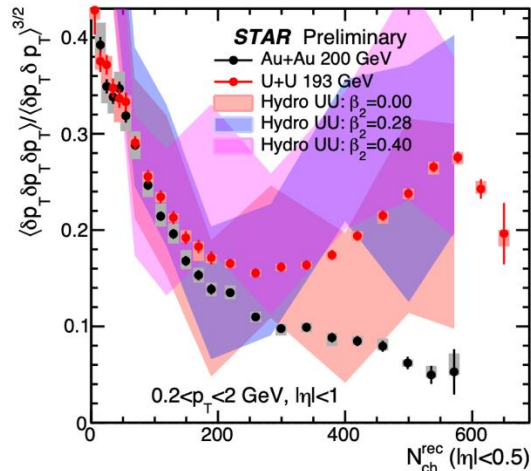
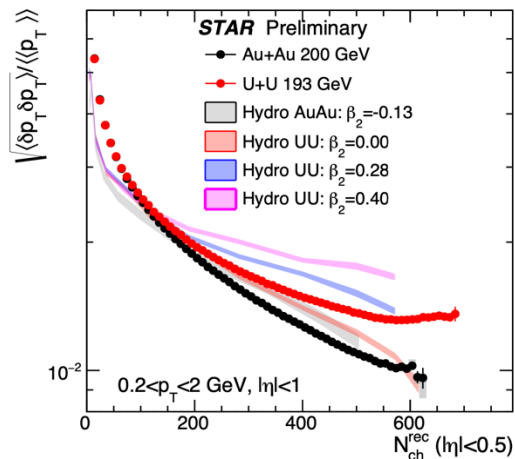


Connecting *ab initio* inputs of light-nuclei with relativistic nuclear collisions

Easier to image the shapes of light-nuclei than symmetric light-ion collisions

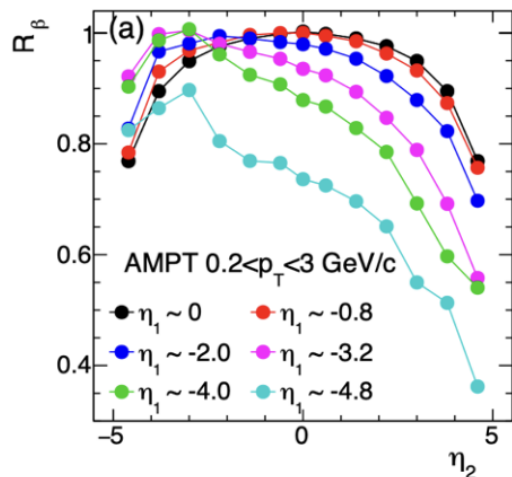
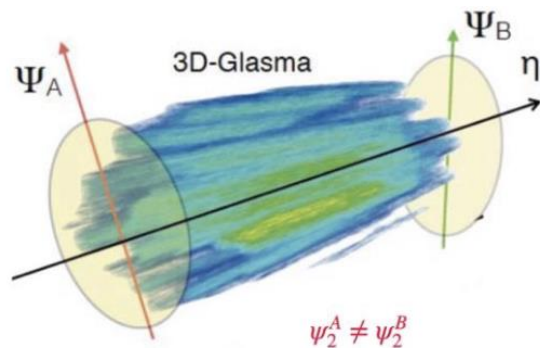
# Other interesting questions remained:

1. More new observables simultaneously constrain nuclear deformation effect



i.e. mean pt fluctuations

2. Beyond the 2D transverse profile of QGP, how the longitudinal structure will be?



$$V_{2\Delta} = V_{2\Delta,sp} + V_{2\Delta,\beta} + \delta_{nf}$$

Isolate the decorrelation map of deformation-induced flow

C. Zhang, S. Huang and J.Jia, 2405.08749

J. Jia, S. Huang, C. Zhang and S. Bhatta, 2408.16006

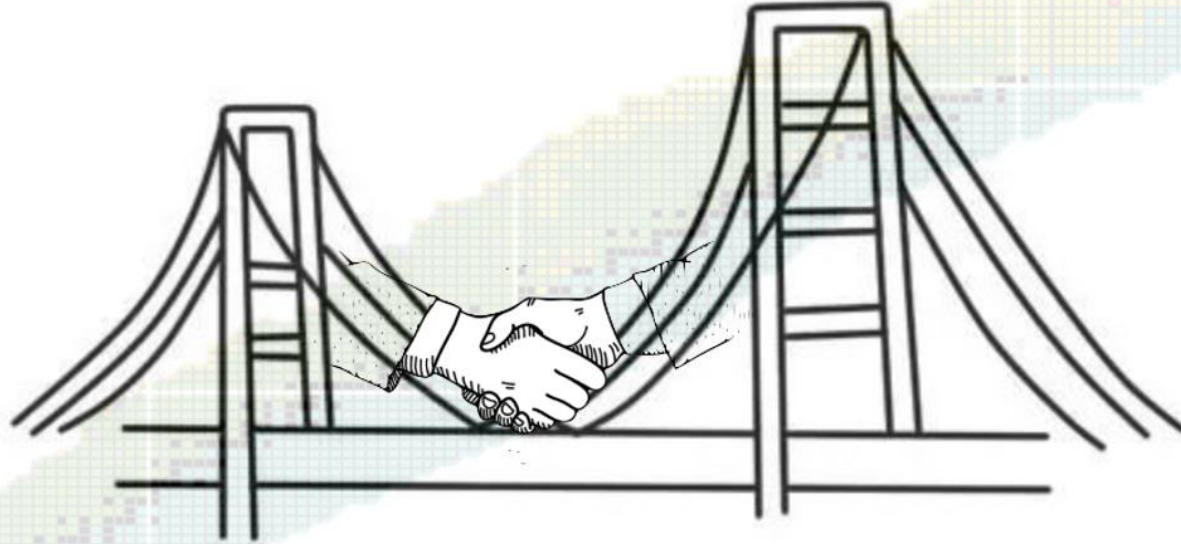
3. Possible new system scan at LHC is helpful to further understand QGP.

- To go beyond simply observing collectivity ( $v_n$ ) in various systems, need measurements that can:
  - Controlled variation of the QGP initial condition
  - understand the nuclear structure across energy scales
- Many potential applications:
  - octupole and hexadecapole nuclear deformations
  - rigid and soft triaxiality (shape fluctuations/coexistence)
  - neutron skin,
  - nuclear cluster in light nuclei
  - neutrinoless double-beta decay
- Interdisciplinary connection between low- and high-energy.

Further constrain the QGP properties and understand the nature of nuclear structure

# *Thank you!*

Low energy community



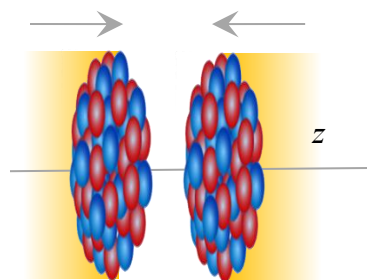
High energy community

I apologize I may not have enough time to cover all important studies...

**Backup**

# Collective flow-assisted nuclear structure imaging

## Nuclear structure



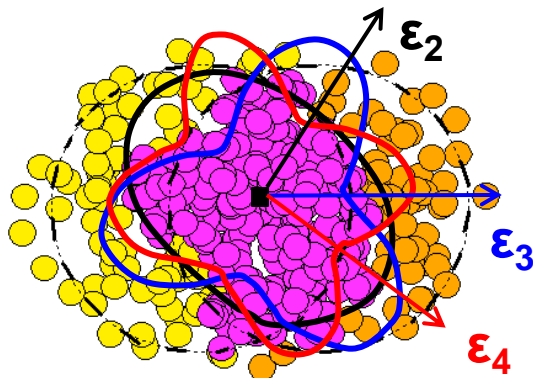
$$\rho(r, \theta, \phi) = \frac{\rho_0}{1 + e^{(r-R(\theta, \phi))/a_0}}$$

$$R(\theta, \phi) = R_0(1 + \beta_2[\cos \gamma Y_{2,0}(\theta, \phi) + \sin \gamma Y_{2,2}(\theta, \phi)] + \beta_3 Y_{3,0}(\theta, \phi))$$

- $\beta_2$  → Quadrupole deformation
- $\beta_3$  → Octupole deformation
- $\gamma$  → Triaxiality
- $a_0$  → Surface diffuseness
- $R_0$  → Nuclear size

Many-body correlations

## Initial conditions



### Initial Size

$$R_{\perp}^2 \propto \langle r_{\perp}^2 \rangle$$

### Initial Shape

$$\mathcal{E}_n \propto \langle r_{\perp}^n e^{in\phi} \rangle$$

$R_0$

$a_0$

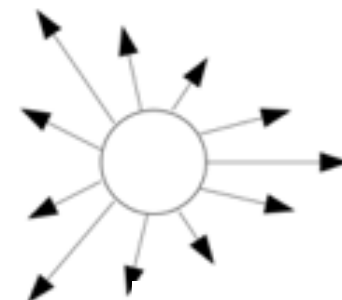
$\beta_n$

?

$$F = -\nabla P(\epsilon)$$

hydro-response

## Final state



### Radial Flow

### Anisotropic Flow

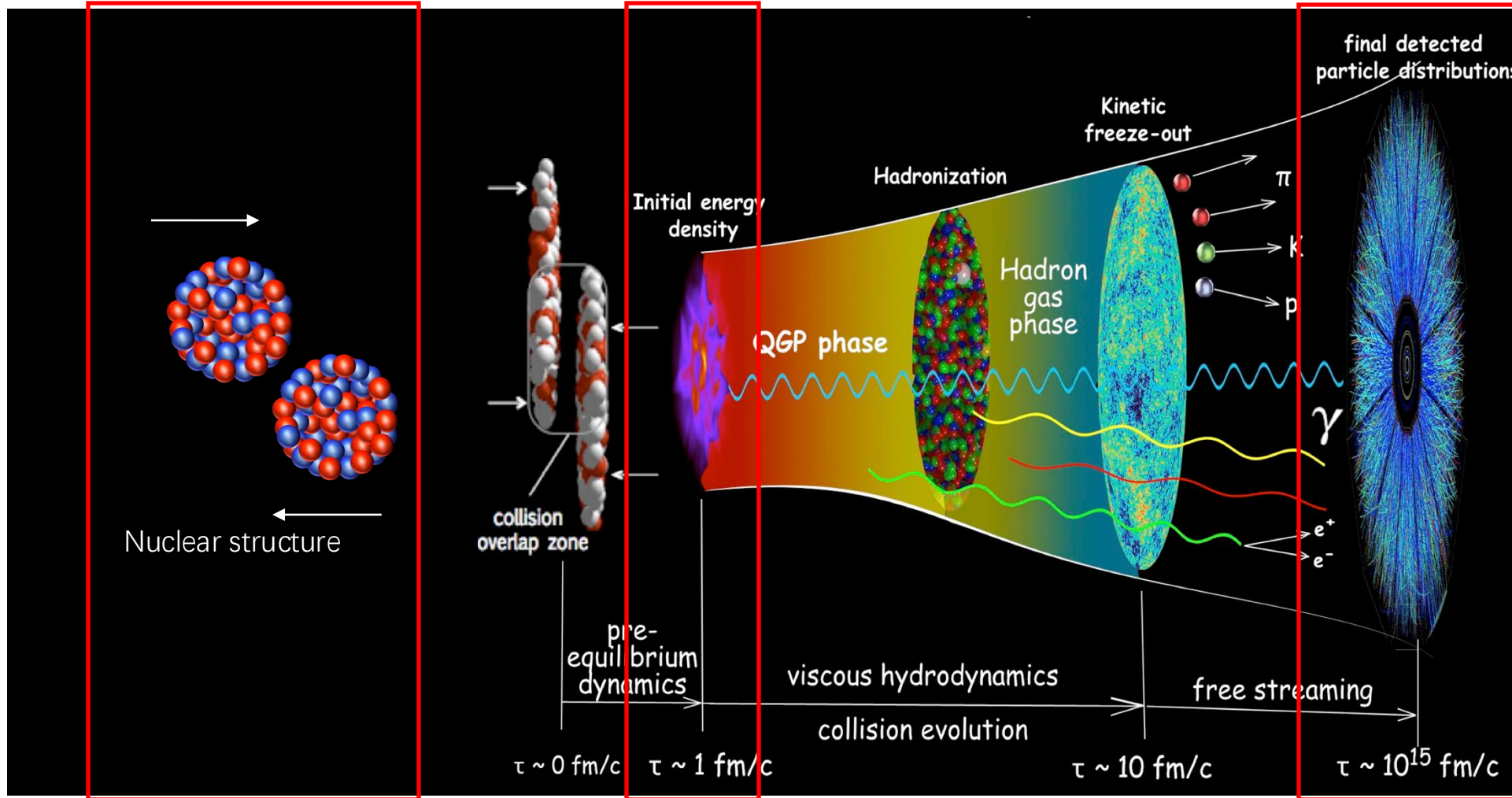
$$\frac{d^2 N}{d\phi dp_T} = N(p_T) \left( \sum_n V_n e^{-in\phi} \right)$$

$$N_{ch} \propto N_{part} \quad \frac{\delta[p_T]}{[p_T]} \propto -\frac{\delta R_{\perp}}{R_{\perp}} \quad V_n \propto \mathcal{E}_n$$

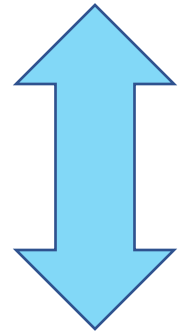
High energy: Large multiplicity and boost invariance; approximate linear response in each event

Constrain the initial condition & Reveal novel properties of nuclei & Study the unknown nuclear structure

# Multi-stages in relativistic heavy-ion collisions



Multiple stage  
/Complex dynamics



Hybrid multi-stage  
Modeling with event-by-  
event fluctuations

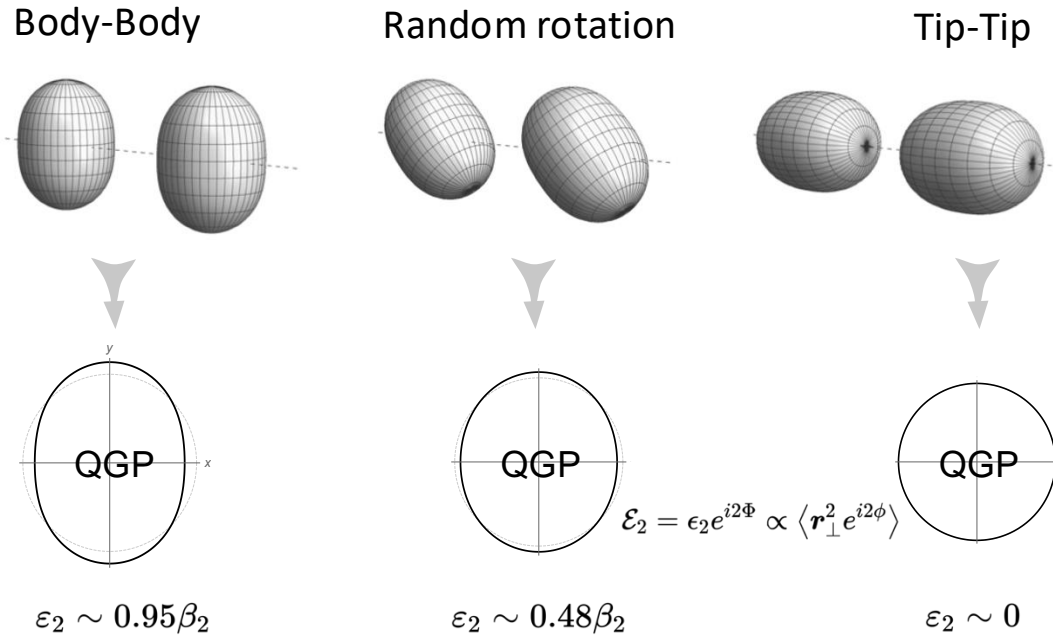
$$\rho(r, \theta, \phi) = \frac{\rho_0}{1 + e^{(r-R(\theta, \phi))/a_0}}$$

$$e(x, y) \sim \begin{cases} \frac{T_A + T_B}{T_A T_B} \\ \sqrt{T_A T_B} \\ \min\{T_A, T_B\} \\ T_A + T_B + \alpha T_A T_B \end{cases}$$

$N_{\text{part}}$  - scaling,  $p = 1$   
 $N_{\text{coll}}$  - scaling,  $p = 0, q = 2$   
 Trento default,  $p = 0$   
 KLN model,  $p \sim -2/3$   
 two-component model,  
 similar to quark-gluon model

$$T \propto \left( \frac{T_A^p + T_B^p}{2} \right)^{q/p}$$

# Connecting the initial conditions to the nuclear shape



$$\epsilon_2 = \underbrace{\epsilon_0}_{\text{undeformed}} + \underbrace{p(\Omega_1, \Omega_2)}_{\text{phase factor}} \beta_2 + \mathcal{O}(\beta_2^2)$$



$$\langle \epsilon_2^2 \rangle \approx \langle \epsilon_0^2 \rangle + 0.2\beta_2^2$$

$$\langle v_n^2 \rangle \propto \langle \epsilon_n^2 \rangle$$

$$\langle (\delta d_{\perp} / d_{\perp})^2 \rangle \sim a_0 + b_0 \beta_2^2 + b_{0,3} \beta_3^2$$

$$\rho(r, \theta, \phi) = \frac{\rho_0}{1 + e^{(r-R(\theta, \phi))/a_0}}$$

$$R(\theta, \phi) = R_0(1 + \beta_2[\cos \gamma Y_{2,0}(\theta, \phi) + \sin \gamma Y_{2,2}(\theta, \phi)] + \beta_3 Y_{3,0}(\theta, \phi))$$

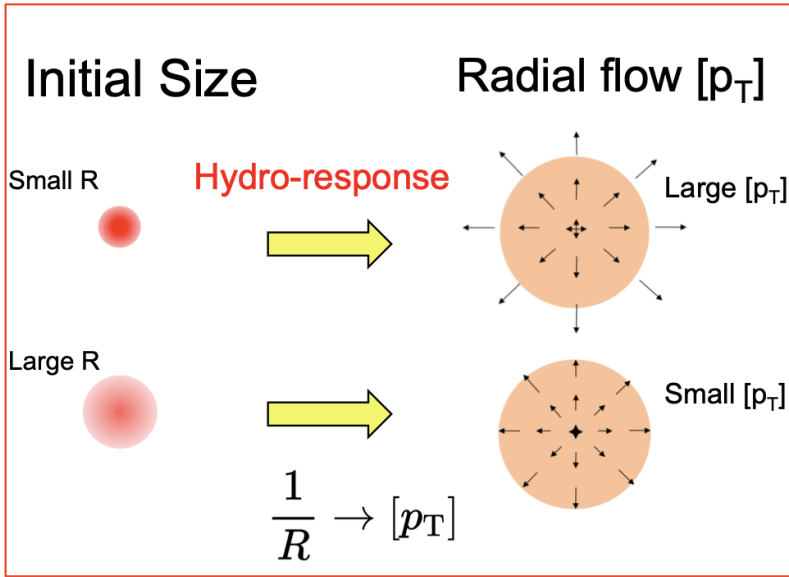
- In principle, can measure any moments of  $\rho(1/R, \epsilon_2, \epsilon_3 \dots)$ 
  - Mean  $\langle d_{\perp} \rangle$
  - Variance  $\langle \epsilon_n^2 \rangle, \langle (\delta d_{\perp} / d_{\perp})^2 \rangle$
  - Skewness  $\langle \epsilon_n^2 \delta d_{\perp} / d_{\perp} \rangle, \langle (\delta d_{\perp} / d_{\perp})^3 \rangle$
  - Kurtosis  $\langle \epsilon_n^4 \rangle - 2\langle \epsilon_n^2 \rangle^2, \langle (\delta d_{\perp} / d_{\perp})^4 \rangle - 3\langle (\delta d_{\perp} / d_{\perp})^2 \rangle^2$
- All have a simple connection to deformation
  - Two-points correlation
  - Three-points correlation

$$\langle \epsilon_2^2 \rangle \sim a_2 + b_{2,2} \langle \beta_2^2 \rangle + b_{2,3} \langle \beta_3^2 \rangle \quad \langle \epsilon_2^2 \delta d_{\perp} / d_{\perp} \rangle \sim a_1 - b_1 \cos(3\gamma) \beta_2^3$$

$$\langle \epsilon_3^2 \rangle \sim a_3 + b_{3,3} \langle \beta_3^2 \rangle + b_{3,4} \langle \beta_4^2 \rangle \quad \langle (\delta d_{\perp} / d_{\perp})^3 \rangle \sim a_2 - b_2 \cos(3\gamma) \beta_2^3$$

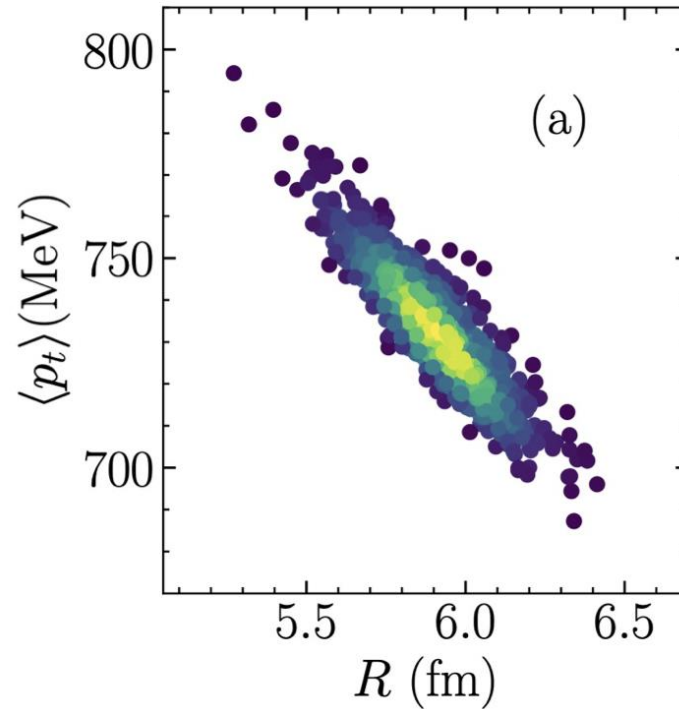
$$\langle \epsilon_4^2 \rangle \sim a_4 + b_{4,4} \langle \beta_4^2 \rangle$$

# Mean transverse momentum [ $p_T$ ] fluctuations

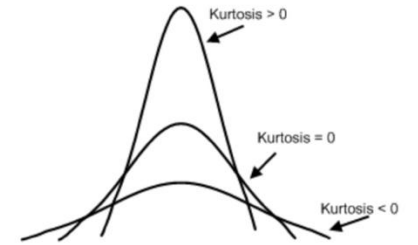
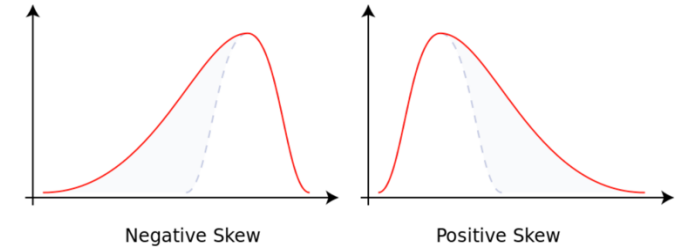


$$\begin{array}{|c|} \hline S_A = S_B \\ \hline R_A < R_B \\ \hline \end{array} \Rightarrow \begin{array}{|c|} \hline T_A > T_B \\ \hline \end{array} \Rightarrow \begin{array}{|c|} \hline \bar{p}_{t,A} > \bar{p}_{t,B} \\ \hline \end{array}$$

Same total energy deposition:  
Smaller transverse size,  
Stronger radial expansion.



$$\delta[p_T] \propto -\delta R \propto \delta d_{\perp}$$



Mean       $\frac{\delta[p_T]}{[p_T]} \propto \frac{\delta d_{\perp}}{d_{\perp}} \propto \beta_2$       J. Jia, PRC105, 044905(2021)

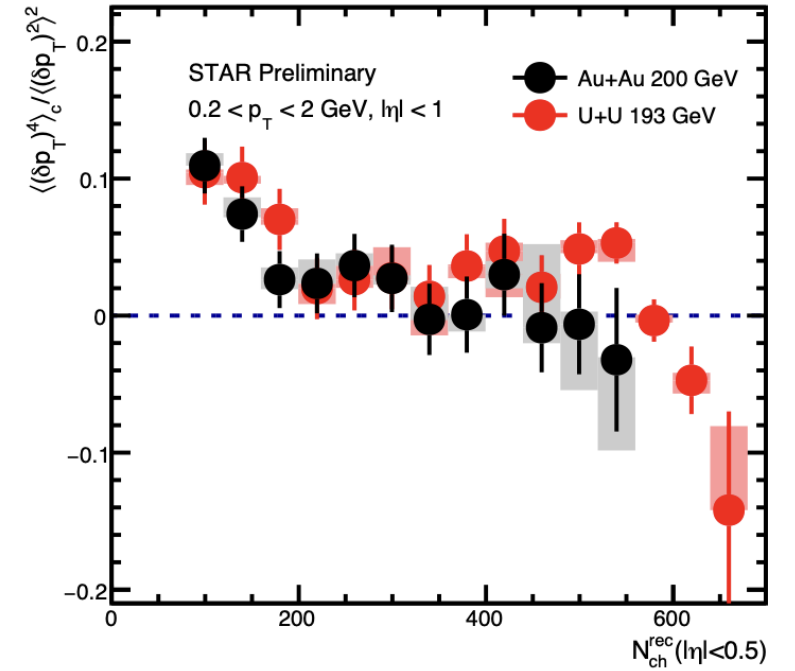
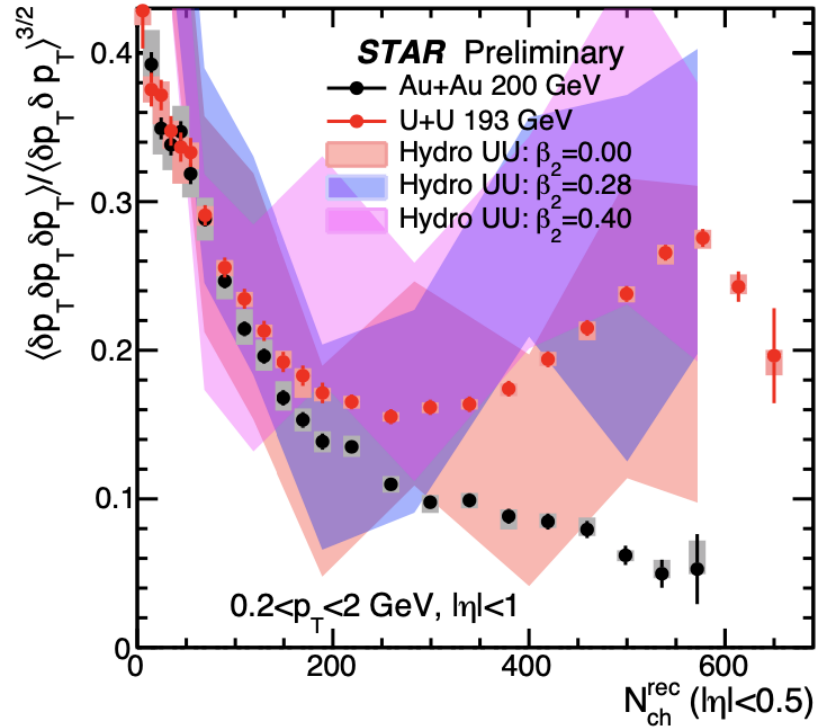
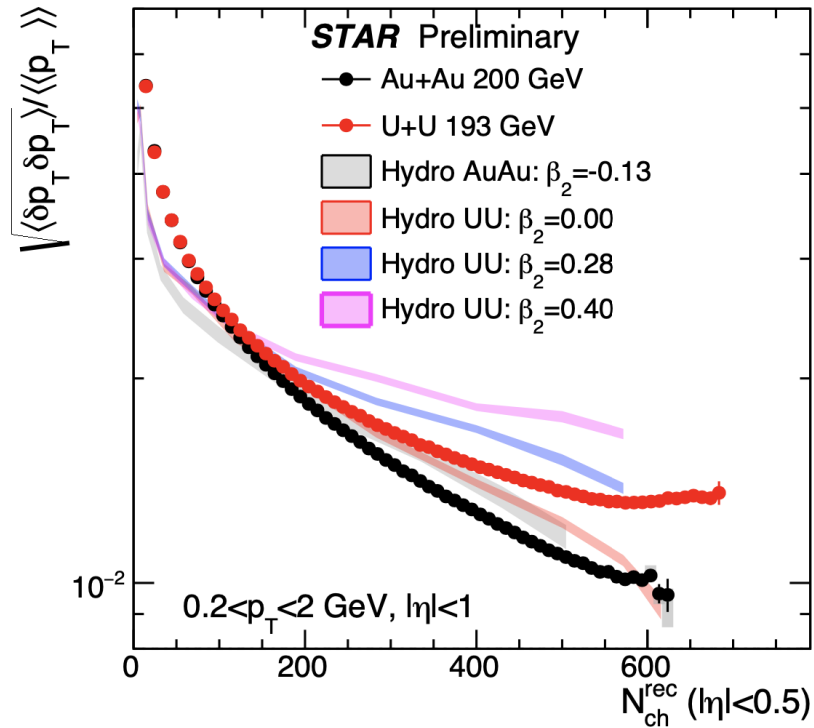
Variance       $\left\langle \left( \frac{\delta[p_T]}{[p_T]} \right)^2 \right\rangle \propto \left\langle \left( \frac{\delta d_{\perp}}{d_{\perp}} \right)^2 \right\rangle \propto \beta_2^2$

Skewness       $\left\langle \left( \frac{\delta[p_T]}{[p_T]} \right)^3 \right\rangle \propto \left\langle \left( \frac{\delta d_{\perp}}{d_{\perp}} \right)^3 \right\rangle \propto \cos(3\gamma) \beta_2^3$

Kurtosis       $\left\langle \left( \frac{\delta[p_T]}{[p_T]} \right)^4 \right\rangle - 3 \left\langle \left( \frac{\delta[p_T]}{[p_T]} \right)^2 \right\rangle^2 \propto \left\langle \left( \frac{\delta d_{\perp}}{d_{\perp}} \right)^4 \right\rangle - 3 \left\langle \left( \frac{\delta d_{\perp}}{d_{\perp}} \right)^2 \right\rangle^2 \propto -\beta_2^4$

Event-by-event [ $p_T$ ] fluctuations also reflect the deformation of colliding nuclei

# [p<sub>T</sub>] fluctuations and comparisons to hydro model



Au+Au: variance and skewness follow independent source scaling  $1/N_s^{n-1}$  within power-law decrease

U+U: large enhancement in normalized variance and skewness and sign-change in normalized kurtosis

→ size fluctuations enhanced

The nuclear deformation role is further confirmed by hydro calculations.

Hydro: private calculations from Bjoern Schenke and Chun Shen

[p<sub>T</sub>] fluctuations also serve as a good observable to explore the role of nuclear deformation.

# Isobar ratios cancel final state effect

- Vary the shear viscosity by changing partonic cross-section
  - Flow signal change by 30-50%, the  $v_n$  ratio unchanged.

C. Zhang, S. Bhatta and J. Jia, PRC106, L031901(2022)

$$v_n = k_n \varepsilon_n$$

↓

$$\frac{v_{n,Ru}}{v_{n,Zr}} \approx \frac{\varepsilon_{n,Ru}}{\varepsilon_{n,Zr}}$$

Robust probe of  
initial state!

